SUPPLEMENTARY MATERIALS

New insights into the binding features of F508del CFTR potentiators: a molecular docking, pharmacophore mapping and QSAR analysis approach

Giada Righetti[1], Monica Casale[2], Michele Tonelli[1], Nara Liessi[3,4], Paola Fossa[1*], Nicoletta Pedemonte[5], Enrico Millo[3,4] and Elena Cichero[1*]

S1. Chemical structures and potency profile of thienopyrazole derivatives **1- 26** as F508del CFTR potentiators [27]. Activity of the compounds was explored by YFP Halide Assay and TECC Experiments[a].

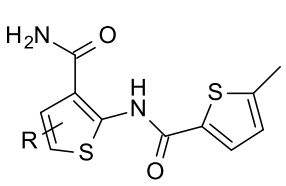

1-3

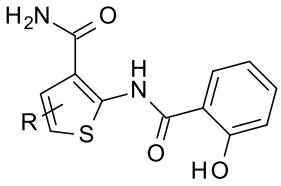

4-6

Compound	R	pEC$_{50}$ M
1	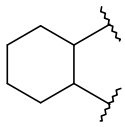	6.18
2	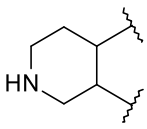	n.a
3	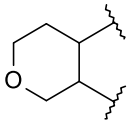	6.10
4	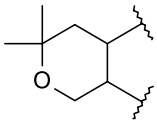	7.88
5	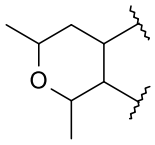	8.39
6	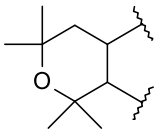	8.39

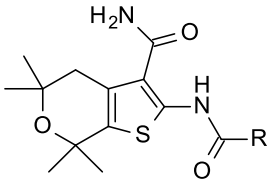

7-26

Cp.	R	pEC_{50} M
7	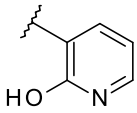	6.72
8	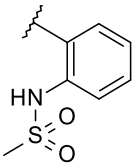	6.83
9	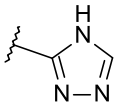	6.33
10	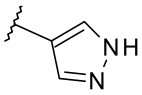	6.90
11	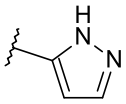	8.52
12	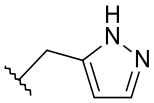	6.86
13	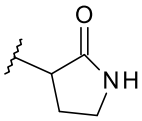	6.99
14	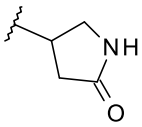	>10,000
15		7.63
16		7.79
17	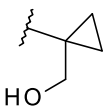	7.82

18	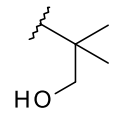	7.12
19	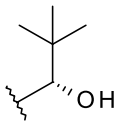	8.56
20	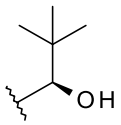	6.89
21	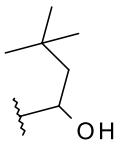	9.26
22	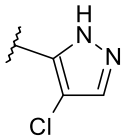	8.69
23	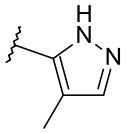	8.69
24	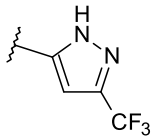	8.52
25	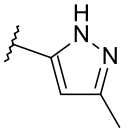	7.88
26	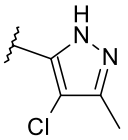	7.95

[a] A bronchial epithelial cell line derived from a CF patient (CFBE41o− cells) was used to overexpress F508delCFTR and yellow fluorescent protein. CFBe41o-cells were cultured in Eagle's Minimal Essential Medium (MEM) (Life Technologies) supplemented with 10% fetal bovine serum (FBS), 1% penicillin/streptomycin, 1% L-glutamine, and 500μg/mL hygromycin B. The cells were grown on culture flasks coated with 0.01% bovine serum albumin (BSA) (Sigma), 30μg/mL Purecol (Nutacon), and 0.001% CFBe41o-human fibronectin (Sigma). CFBe41o-cells were transduced with adenoviruses containing F508delCFTRand YFP (H148Q/I152L/F47L). Then, CFBE41o− cells were incubated for 24 h at 27 °C and treated for 10 min with 10 μM forskolin and the desired concentration of potentiator at room temperature. The YFP fluorescence was recorded during 7 s (CFBE41o−) starting immediately before addition of NaI buffer to the wells, using a fluorescence reader. Transepithelial clamp circuit (TECC) recordings were performed using the TECC instrument developed and sold by EP Design (Bertem, Belgium). For acute potentiator experiments, compounds were added on both sides to test their potential for increasing CFTR gating. Measurements were done during a 20min time frame with recordings every 2min. The transepithelial potential (PD) and transepithelial resistance

(Rt) were measured in an open circuit and transformed to I_{eq} using Ohm's law. The increase in I_{eq} (ΔI) was used as a measure for the increased CFTR activity.The capacity of potentiator to increase CFTR channel function was expressed as 1-(fluorescence after NaI addition (F)/fluorescence before NaI addition (F0)).

S2. Chemical structures and potency profile of cyanoquinolines **27- 32** as F508del CFTR potentiators [28]. Potentiator activity is assayed in low-temperature rescued F508del-CFTR-expressing cells in which the protein is targeted to the plasma membrane by 12-h incubation at reduced temperature, and test compound (together with cAMP agonist) is added just before or at the time of fluorescence or electrophysiological assay.[a.]

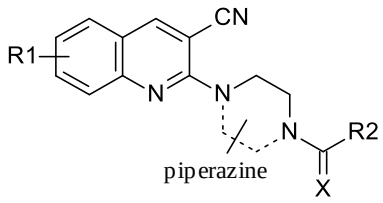

Compound	Structure	pEC50 M
27	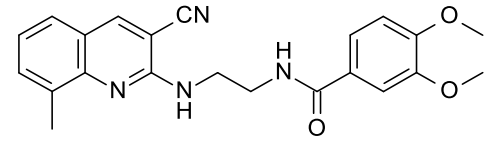	4.82
28	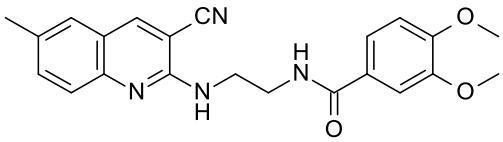	4.82
29	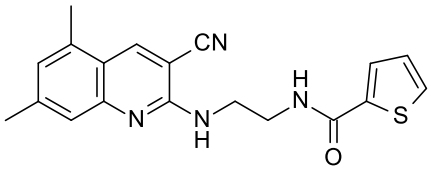	4.85
30	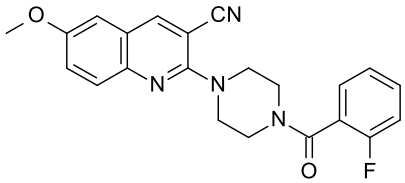	4.95
31	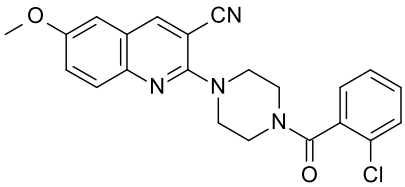	5.33
32	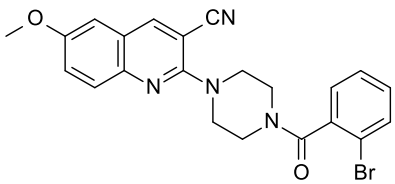	5.30

[a] Fisher rat thyroid (FRT) epithelial cells were stably transfected with F508del-CFTR. The CFTR-expressing cell lines was also transfected with halide-sensitive green fluorescent protein YFP-H148Q/I152L/F46L. For

potentiator assay, FRT cells were grown at 37°C/5% CO2 for 18 to 24 h and then for 18 to 24 h at 27°C. At the time of the assay, cells were washed with PBS and then incubated for 10 min with PBS (50 µl) containing forskolin (20 µM) and test compound (0–25 µM final concentration). each well was assayed individually for I^- influx by recording fluorescence continuously (200 ms per point) for 2 s (baseline) and then for 12 s after rapid addition of 165 µl of PBS, in which 137 µM Cl^- was replaced by I^-. All compound plates contained negative controls (DMSO vehicle) and positive controls (50 µM genistein for potentiator assay).

S3. Chemical structures and potency profile of cyanoquinolines **33-56** as F508del CFTR potentiators[a] [29].

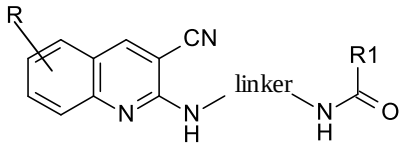

Compound	Structure	pEC_{50} M
33	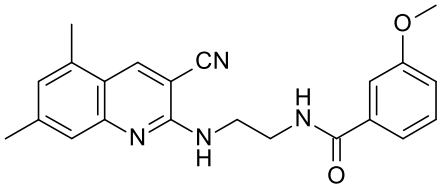	5.22
34	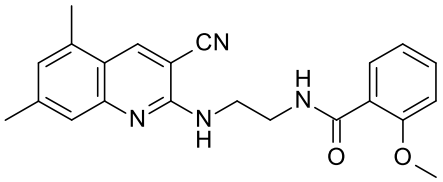	5.63
35	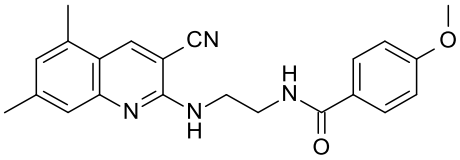	5.38
36	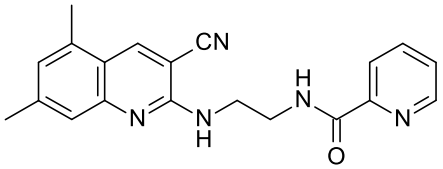	5.92
37	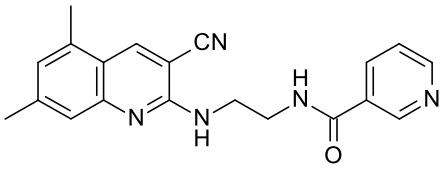	4.87
38	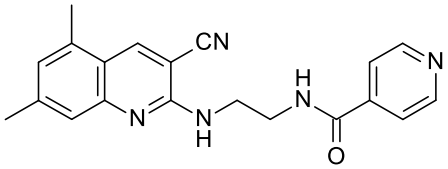	5.00

39	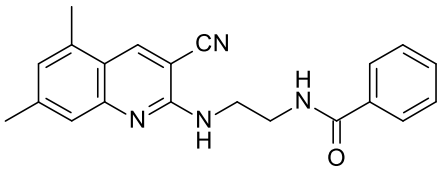	5.00
40	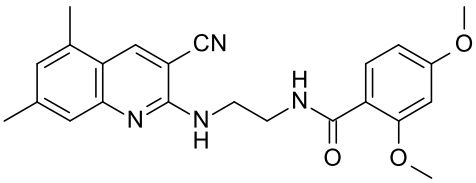	4.25
41	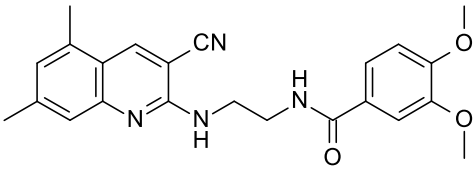	4.31
42	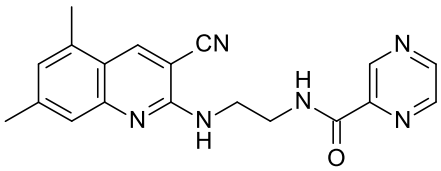	n.a
43	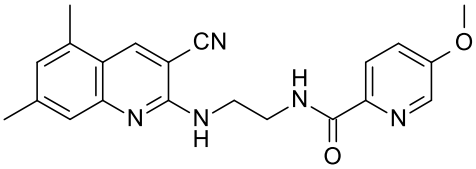	5.46
44	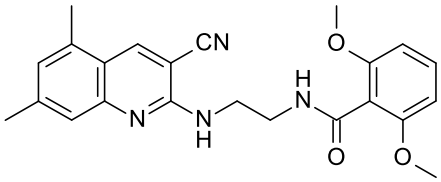	4.93
45	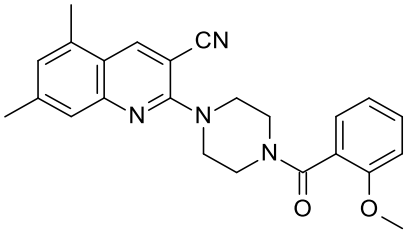	6.00
46	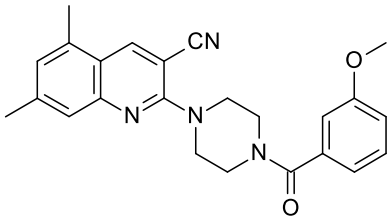	5.92

47	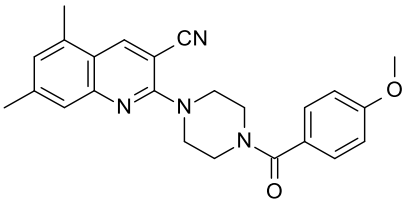	5.88
48	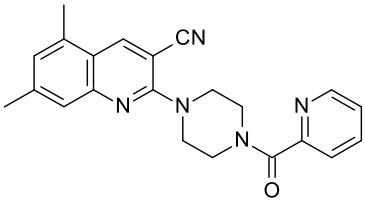	5.13
49	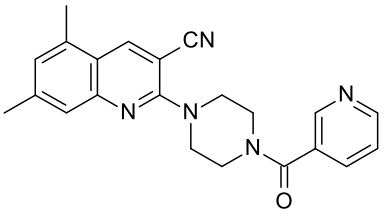	n.a
50	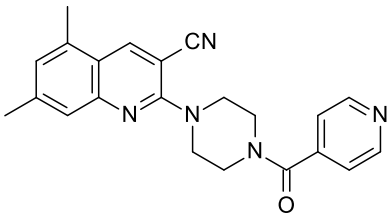	n.a
51	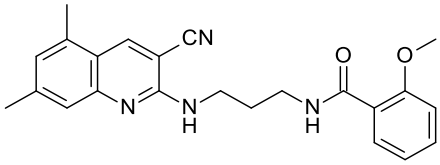	4.55
52	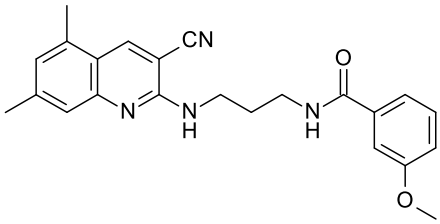	5.33
53	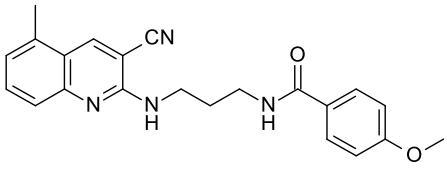	5.30
54	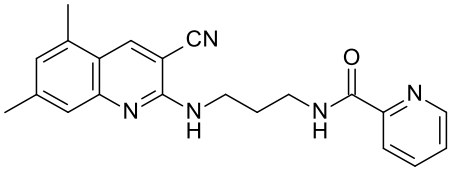	5.21

55	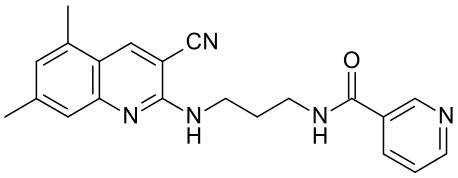	4.79
56	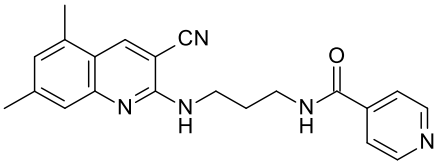	4.87

[a] For potentiator assay, cells were grown at 37 °C for 18–24 h and then for 18–24 h at 27 °C. At the time of the assay, cells were washed with PBS and then incubated for 10 min with PBS (50 μL) containing forskolin (20 μM) and test compound (0–50 μM final concentration). Measurements were carried out using FLUOstar fluorescence plate readers (Optima, BMG LABTECH Gmbh). Each well was assayed individually for I− influx by recording fluorescence for 2 s (baseline) and then for 12 s after rapid addition of 165 μL of PBS in which 137 mM Cl− was replaced by I−. I− influx rate was computed by exponential regression. All experiments contained negative control (DMSO vehicle) and positive controls (potentiator assay, genistein). EC_{50} and Vmax, and their associated uncertainties, were determined by 4 parameter logistic nonlinear regression from concentration-activity data using GraphPad Prism Version 5.01.

S4. Chemical structures and potency profile of piperidine-pyridoindole analogs **57-69** as F508del CFTR potentiators[a] [26].

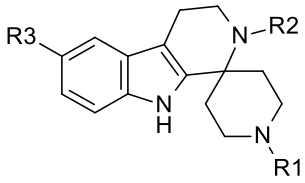

Compound	R_1	R_2	R_3	pEC_{50} M
57	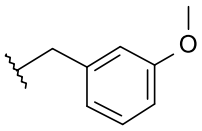	H	OMe	5.00
58	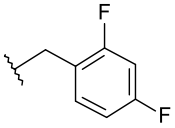	H	OMe	5.69
59	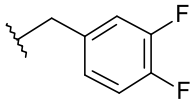	H	OMe	5.58
60	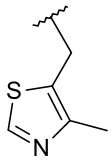	H	OMe	5.29
61	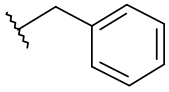	H	H	4.79

62	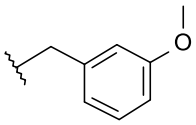	H	H	4.88
63	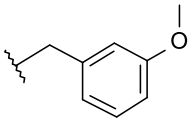	Me	H	< 4.52
64	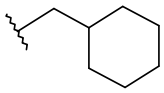	H	OMe	< 4.52
65	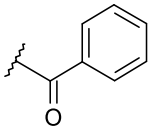	H	H	< 4.52
66	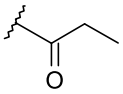	H	OMe	< 4.52
67	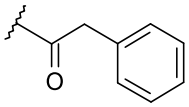	H	OMe	< 4.52
68	SO_2Me	H	OMe	< 4.52
69	Me	H	OMe	< 4.52

[a] Screening of potentiators was done using FRT cells stably expressing different mutant of the CFTR protein and the halide-sensitive EYFP-H148Q/I152L/F46L (YFP) that were treated for 24 hours with 3 μM VX-809 to increase CFTR1281 cell surface expression. Just prior to assay cells were treated for 10 min with test compounds at 25 μM together with 20 μM forskolin and 15 nM VX-770. CFTR channel activity was deduced from the initial rate of YFP fluorescence quenching in response to addition of iodide-substituted phosphate buffered saline. After initial confirmation with plate reader assays, short-circuit current measurement revealed the most promising derivatives. .

S5. Chemical structures and chemical compounds of pyrazoloquinolines analogs **70-80** as F508del CFTR potentiators[a] [26].

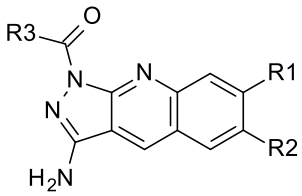

Compound	R_1	R_2	R_3	pEC_{50} M
70	OMe	H	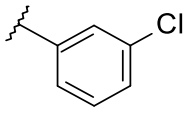	4.82
71	OMe	H	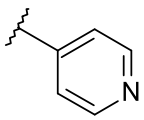	< 4.52

72	OMe	H	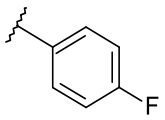	5.44
73	OMe	H	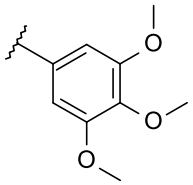	< 4.52
74	OMe	H	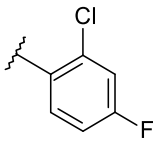	5.61
75	OMe	H	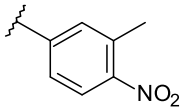	< 4.52
76	OMe	H	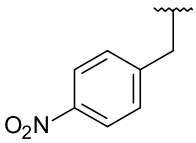	< 4.52
77	OMe	H	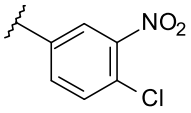	< 4.52
78	OMe	H	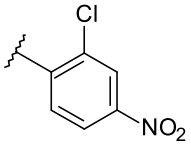	5.76
79	OMe	H	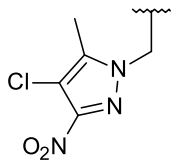	< 4.52
80	OMe	H	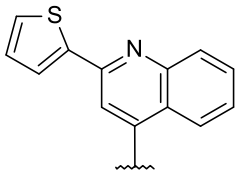	6.52

[a] Screening of potentiators was done using FRT cells stably expressing different mutant of the CFTR protein and the halide-sensitive EYFP-H148Q/I152L/F46L (YFP) that were treated for 24 hours with 3 μM VX-809 to increase CFTR1281 cell surface expression. Just prior to assay cells were treated for 10 min with test compounds at 25 μM together with 20 μM forskolin and 15 nM VX-770. CFTR channel activity was deduced from the initial rate of YFP fluorescence quenching in response to addition of iodide-substituted phosphate buffered saline. After initial confirmation with plate reader assays, short-circuit current measurement revealed the most promising derivatives. .

S6. Chemical structures and potency profile of aminoarylthiazoles **81-88** as F508del CFTR potentiators[a] [22-23].

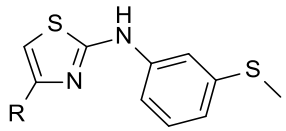

Compound	R	pEC_{50} M
81	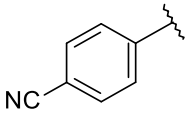	4.46
82	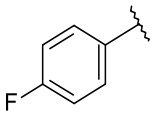	4.56
83	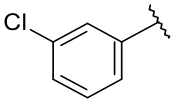	4.27
84	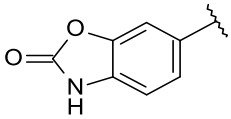	5.19
85	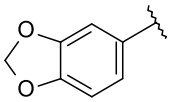	4.14
86	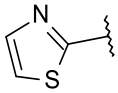	5.00
87	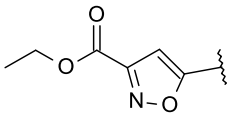	4.23
88	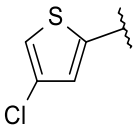	4.49
89	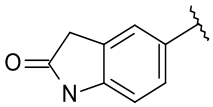	5.71
90	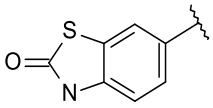	5.20

[a] For determination of potentiator activity on F508del-CFTR, CFBE41o-cells were incubated for 24 h at 27 °C to allow trafficking of the mutant protein to plasma membrane. Cells were then stimulated with for 30 min with PBS containing forskolin (20 μM) plus the compound to be tested at the desired concentration. For determination of potentiator activity on G551D-CFTR, FRT cells were directly stimulated with forskolin plus compound cocktail without previous incubation at low temperature.

S7. Superimposition of the X-ray crystallographic data of CFTR in complex with **VX-770** (pdb code = 6O2P; ribbon in light blue.) and with **GLPG1837** (pdb code = 6O1V; ribbon in pink.). [21]

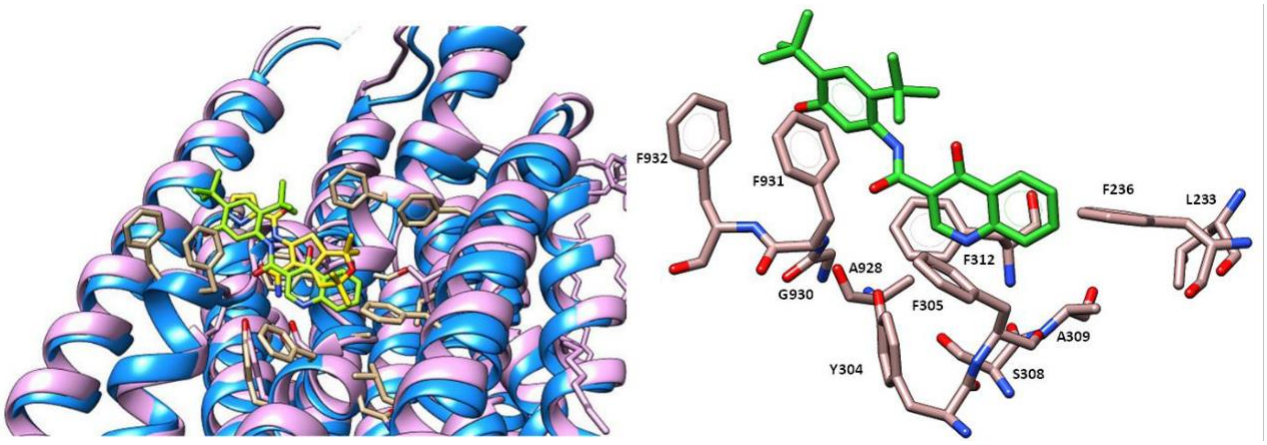

S8. Predicted binding affinity values and related scoring functioning obtained by molecular docking studies of the compounds VX-770 and GLPG-1837 by means of LeadIT software.

hCFTR-Potentiator Complex (LeadIT)	Binding Affinity Energy ΔG (kJ/mol)	Score
hCFTR-VX-770	-20.0	-24.5839
hCFTR-GLPG1837	-13.0	-25.0793

S9. Predicted binding affinity values and related scoring functioning obtained by molecular docking studies of thienopyrane derivatives **1-26** by means of LeadIT software.

.

hCFTR-Potentiator Complex (LeadIT)	Binding Affinity Energy ΔG (kJ/mol)	Score
hCFTR-1	-27.0	-22.8042
hCFTR-2	-24.0	-22.0944
hCFTR-3	-24.0	-21.9986
hCFTR-4	-16.0	-20.2080
hCFTR-5	-13.0	-18.2435
hCFTR-6	-18.0	-22.5589
hCFTR-7	-16.0	-23.8179
hCFTR-8	-15.0	-23.7156
hCFTR-9	-13.0	-20.2545
hCFTR-10	-17.0	-24.3329
hCFTR-11	-19.0	-23.3311
hCFTR-12	-17.0	-20.1142
hCFTR-13	-15.0	-21.3397
hCFTR-14	-17.0	-22.2725
hCFTR-15	-16.0	-18.5975
hCFTR-16	-18.0	-20.5363
hCFTR-17	-19.0	-18.0243
hCFTR-18	-18.0	-17.6943
hCFTR-19	-20.0	-19.9937
hCFTR-20	-18.0	-19.1455
hCFTR-21	-18.0	-17.8490
hCFTR-22	-16.0	-25.0372
hCFTR-23	-17.0	-24.6190
hCFTR-24	-18.0	-20.7271
hCFTR-25	-16.0	-25.9844
hCFTR-26	-16.0	-23.8951

S10. Predicted binding affinity values and related scoring functioning obtained by molecular docking studies of the cyanoquinoline derivatives **27-56** by means of LeadIT software.

hCFTR-Potentiator Complex (LeadIT)	Binding Affinity Energy ΔG (kJ/mol)	Score
hCFTR-27	-17.0	-16.9254
hCFTR-28	-13.0	-13.3363
hCFTR-29	-10.0	-17.2431
hCFTR-30	-13.0	-17.9474
hCFTR-31	-19.0	-17.1064
hCFTR-32	-11.0	-15.8932
hCFTR-33	-16.0	-16.1000
hCFTR-34	-13.0	-15.9863
hCFTR-35	-9.0	-16.2100
hCFTR-36	-21.0	-16.5779
hCFTR-37	-12.0	-17.2708
hCFTR-38	-21.0	-15.9125
hCFTR-39	-24.0	-16.7263
hCFTR-40	-17.0	-12.1516
hCFTR-41	-11.0	-10.7610
hCFTR-42	-14.0	-15.3367
hCFTR-43	-20.0	-14.4144
hCFTR-44	-9.0	-10.5040
hCFTR-45	-22.0	-20.1247
hCFTR-46	-17.0	-20.9311
hCFTR-47	-23.0	-19.7379
hCFTR-48	-19.0	-18.2752
hCFTR-49	-9.0	-18.6320
hCFTR-	-21.0	-19.5051

S11. Predicted binding affinity values and related scoring

50		
hCFTR-51	-13.0	-15.0328
hCFTR-52	-18.0	-14.8880
hCFTR-53	-11.0	-12.3257
hCFTR-54	-10.0	-14.7449
hCFTR-55	-21.0	-15.4514
hCFTR-56	-28.0	-14.9877

functioning obtained by molecular docking studies of the piperidine-pyridoindole derivatives **57-69** by means of LeadIT software.

.

hCFTR-Potentiator Complex (LeadIT)	**Binding Affinity Energy ΔG (kJ/mol)**	**Score**
hCFTR-57	-28.0	-13.5717
hCFTR-58	-25.0	-14.9293
hCFTR-59	-33.0	-13.2128
hCFTR-60	-31.0	-13.6552
hCFTR-61	-31.0	-12.4418
hCFTR-62	-34.0	-12.9565
hCFTR-63	-16.0	-9.9620
hCFTR-64	-36.0	-15.5064
hCFTR-65	-16.0	-14.9051
hCFTR-66	-32.0	-15.1299
hCFTR-67	-33.0	-15.3735
hCFTR-68	-30.0	-14.7068
hCFTR-69	-29.0	-14.0463

S12. Predicted binding affinity values and related scoring functioning obtained by molecular docking studies of the pyrazoloquinolines derivatives **70-80** by means of LeadIT software.

hCFTR-Potentiator Complex (LeadIT)	Binding Affinity Energy ΔG (kJ/mol)	Score
hCFTR-70	-21.0	-23.6952
hCFTR-71	-20.0	-24.9928
hCFTR-72	-10.0	-22.0682
hCFTR-73	-21.0	-18.2053
hCFTR-74	-22.0	-23.3145
hCFTR-75	-19.0	-23.1269
hCFTR-76	-24.0	-24.4577
hCFTR-77	-12.0	-21.6711
hCFTR-78	-11.0	-22.3452
hCFTR-79	-8.0	-25.5199
hCFTR-80	-12.0	-21.1932

S13. Predicted binding affinity values and related scoring functioning obtained by molecular docking studies of the AATs **81-90** by means of LeadIT software.

hCFTR-Potentiator Complex (LeadIT)	Binding Affinity Energy ΔG (kJ/mol)	Score
hCFTR-81	-17.0	-16.2965
hCFTR-82	-24.0	-21.7077
hCFTR-83	-24.0	-22.0010
hCFTR-84	-23.0	-20.1156
hCFTR-85	-25.0	-21.6964
hCFTR-86	-20.0	-19.0612
hCFTR-87	-29.0	-13.0829
hCFTR-88	-22.0	-19.0818
hCFTR-89	-21.0	-17.6904
hCFTR-90	-24.0	-19.1025

S14. Ligplot of the derived poses of docking compound **11** (left) and **22**, **23** (right) at the CFTR cavity.

S15. Ligplot of the derived docking poses of compound **11** (left) and **10**, **12** at the CFTR cavity.

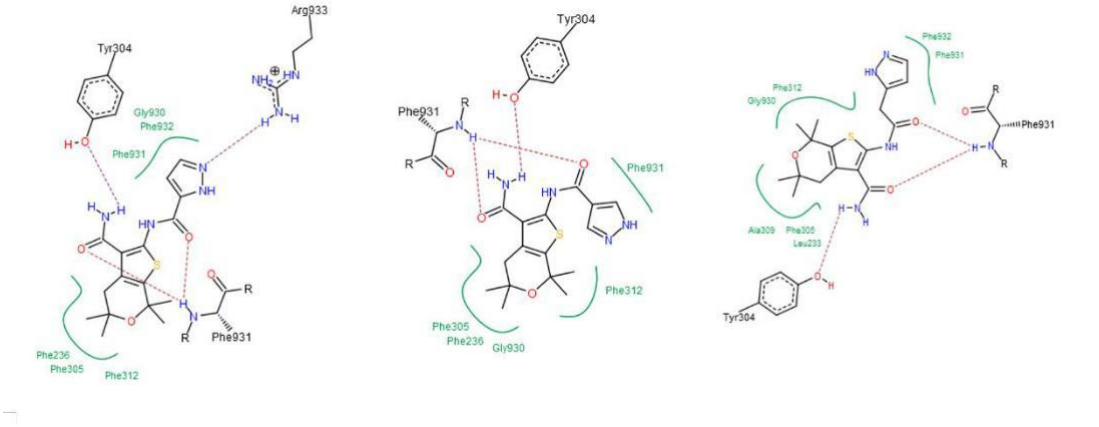

S16. Ligplot of the derived docking poses of compound **9** *(left)* and **12 (***right)* at the CFTR cavity.

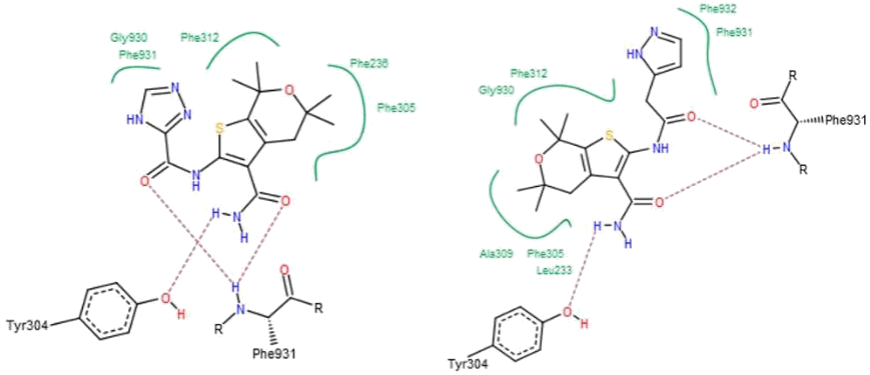

S17. Docking positioning of compound **19** (*left*; *C* atom in deep pink) and of compound **20** (*right*; *C* atom in green) within the human CFTR protein.

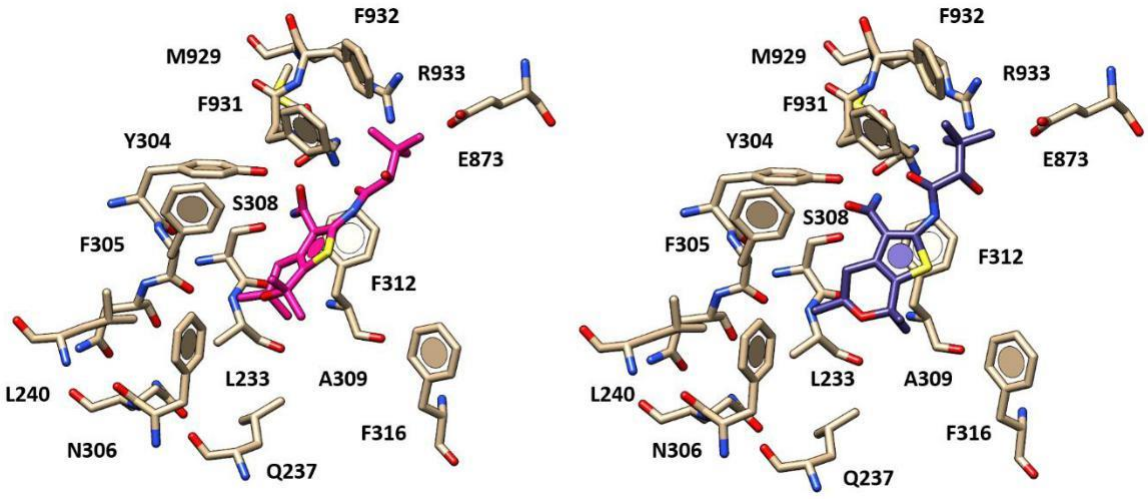

S18. Docking positioning of the compound **21** *S* enantiomer (*C* atom; yellow) within the human CFTR protein.

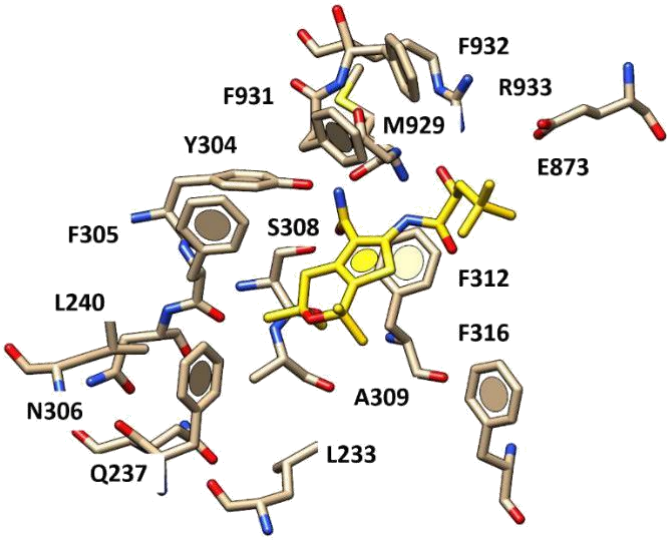

S19. Ligplot of the derived docking poses of compound **45** *(left)* and **48 (***right)* at the CFTR cavity.

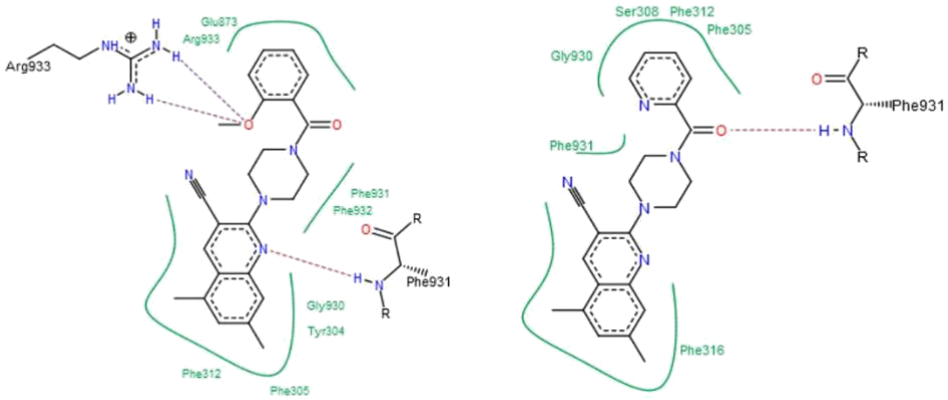

S20. Docking positioning of compound **34** (*C* atom; pink) compared to that of compound **45** (*C* atom; light green) within the human CFTR protein.

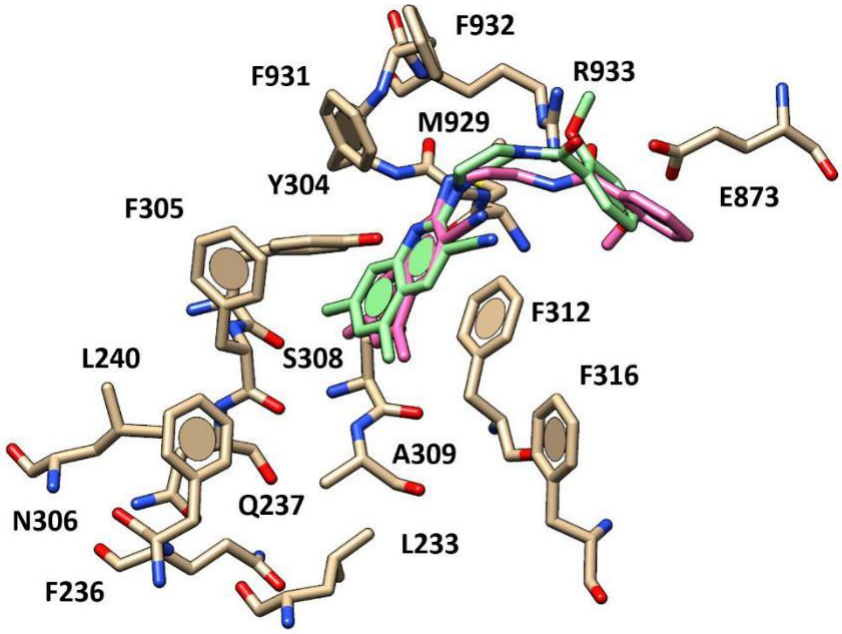

S21. Docking positioning of compound **31** (*C* atom; yellow) compared to that of compound **45** (*C* atom; light green) within the human CFTR protein.

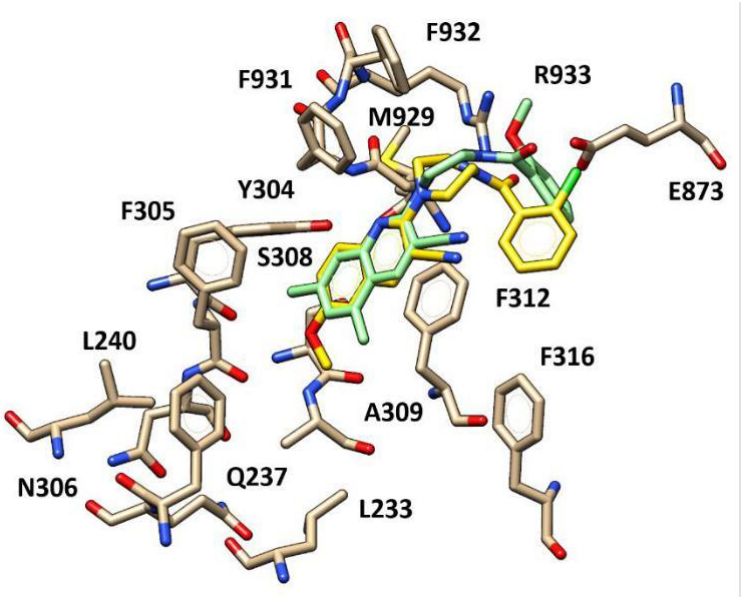

S22. Ligplot of the derived docking poses of compound **62** *(left)* and **67**, **64** **(***right; upper and lower side)* at the CFTR cavity.

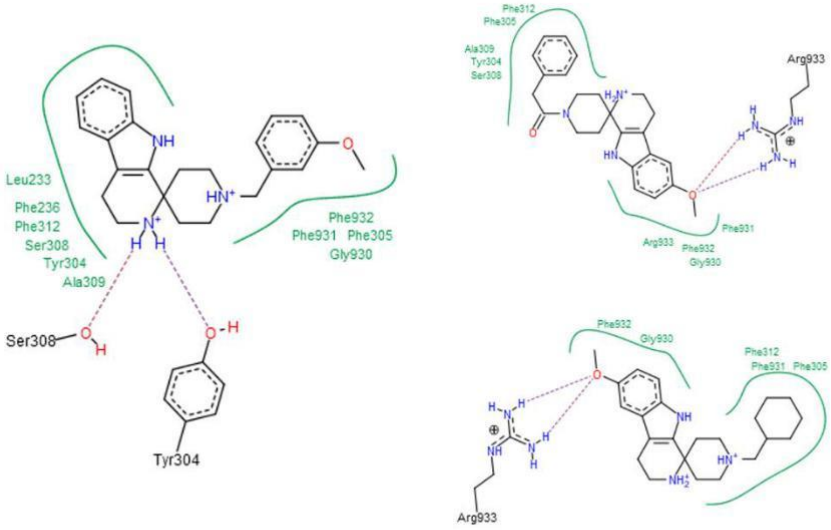

S23. Docking positioning of compound **80** (*C* atom; green) within the X-ray crystallographic structure of the human CFTR in presence of the docked VX-770 (*C* atom; magenta).

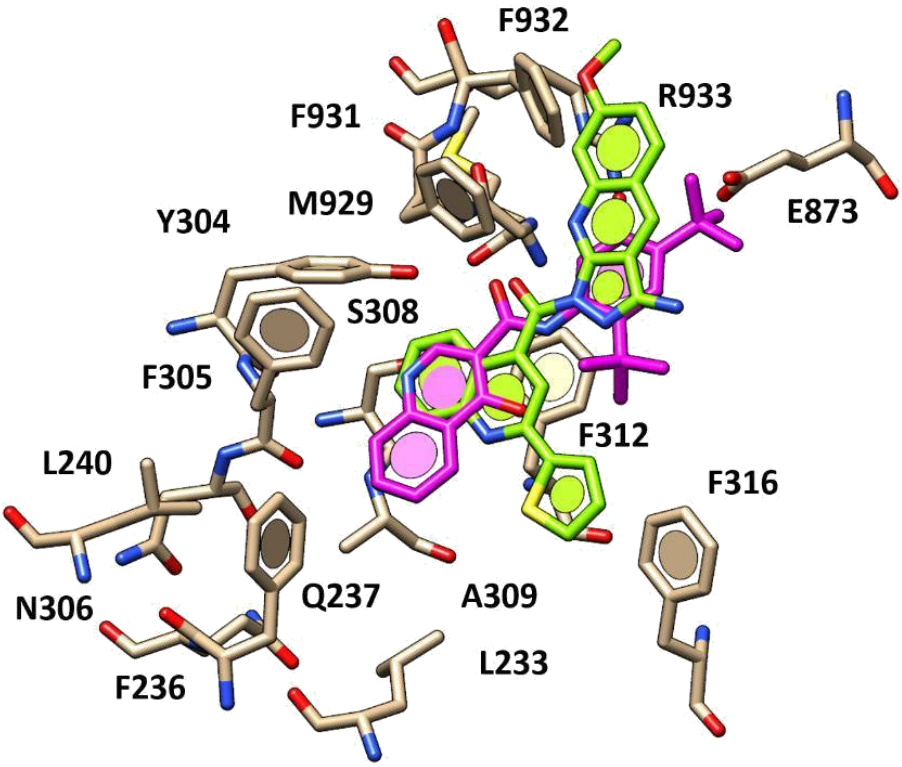

S24. Alignment of derivatives **1**-**26** used for the development of the pharmacophore model. Compound **11** has been used as reference ligand.

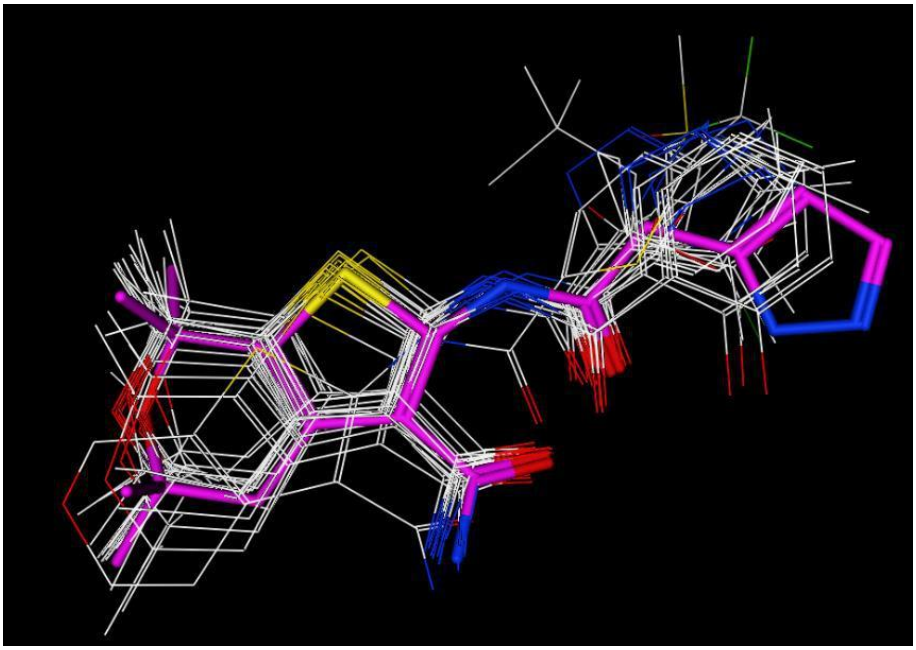

S25. Distanced among the pharmacophore features exhibited by at least the 80% of the thieno-containing derivatives **1**-**26**, acting as CFTR potentiators.

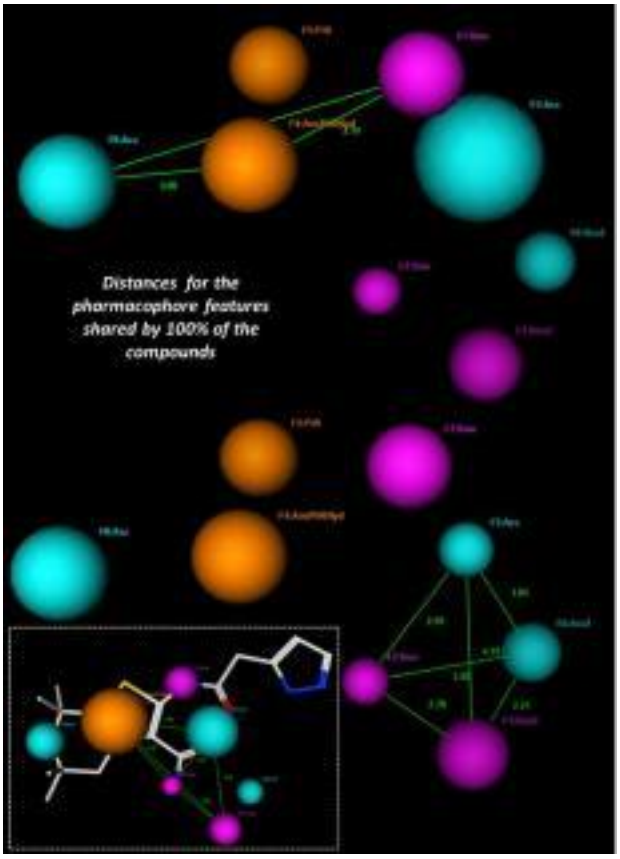

S26. Experimental (Exp.pEC_{50}) and predicted (Pred.pEC_{50}) values of the training set compounds according to the developed QSAR model. The selected 2D Adjacency and Distance Matrix Descriptors, Pharmacophore Feature Descriptors, Physical Properties, Atom Counts and Bond Counts descriptors and the 3D Conformation Dependent Charge Descriptors values have been reported.

Cp.	Exp. pEC_{50}	BCUT_SLOGP_1	BCUT_SMR_1	BCUT_SMR_2	BCUT_SMR_3	b_1rotR	logS	dipoleY	a_hyd	ASA+	Pred. pEC_{50}	Residual
1	6.18	-0.35568	-0.28266	0.798257	2.883142	0.130435	-4.78087	1.204581	15	371.5502	6.12	0.0584
4	7.88	-0.32796	-0.25849	0.652405	2.905984	0.12	-4.79947	1.044069	16	390.8534	7.32	0.5626
7	6.72	-0.35712	-0.26889	0.656855	2.955143	0.107143	-4.025	0.745493	16	382.3849	6.94	-0.2237
8	6.83	-0.34052	-0.25029	0.62132	2.955196	0.15625	-4.22493	1.129376	17	390.6831	6.59	0.2433
9	6.33	-0.34229	-0.26413	0.633213	2.955108	0.115385	-3.76415	0.740564	12	340.8268	6.95	-0.6186
10	6.90	-0.24732	-0.14753	0.604097	2.955141	0.115385	-3.76987	0.922183	15	354.6852	7.36	-0.4613
12	6.86	-0.25409	-0.13852	0.544934	2.955387	0.148148	-3.98426	0.652829	16	374.0897	7.08	-0.2195
22	8.69	-0.24278	-0.14413	0.618789	2.955143	0.111111	-4.65708	0.762706	16	386.3489	8.07	0.6208
23	8.69	-0.12432	-0.0424	0.496516	2.95516	0.111111	-4.08326	0.870343	16	369.6105	8.03	0.6621
25	7.88	-0.21336	-0.11747	0.566128	2.955142	0.111111	-4.23618	0.861456	16	389.3108	7.90	-0.0228
26	7.95	-0.19151	-0.06593	0.597892	2.95515	0.107143	-4.97047	0.794395	17	413.9033	8.50	-0.5481
27	4.82	-0.54106	-0.41293	0.753114	2.741984	0.225806	-4.63377	-0.6466	19	352.3749	4.31	0.5125
28	4.82	-0.57448	-0.41224	0.756553	2.741531	0.225806	-4.94722	-0.54837	19	373.7593	4.60	0.2203
29	4.85	-0.47238	-0.41315	0.724984	2.741931	0.185185	-5.12705	-0.83096	17	348.8117	5.18	-0.3335
33	5.22	-0.51784	-0.38127	0.74058	2.741941	0.2	-5.37076	0.008091	19	368.5545	5.48	-0.2638
30	4.95	-0.51287	-0.423	0.763975	2.924864	0.125	-4.8917	0.258115	20	329.1659	5.12	-0.1726

31	5.53	-0.47932	-0.38118	0.7931	2.925107	0.125	-5.33101	0.229203	20	374.0451	5.37	0.1581
34	5.63	-0.50703	-0.40016	0.750418	2.742956	0.2	-5.37076	-0.19278	19	365.1611	5.51	0.1183
35	5.38	-0.51276	-0.37429	0.73428	2.741745	0.2	-5.37076	-0.11834	19	368.825	5.22	0.1587
36	5.92	-0.47947	-0.40816	0.738283	2.739221	0.178571	-4.21516	-0.32604	17	333.2777	5.14	0.7827
37	4.87	-0.50561	-0.41076	0.752206	2.740608	0.178571	-4.06224	-0.05267	17	314.3405	5.14	-0.2747
39	5.00	-0.53808	-0.43228	0.76661	2.741382	0.178571	-5.32038	-0.11748	18	336.9756	5.18	-0.1837
41	4.31	-0.50842	-0.323	0.720619	2.742418	0.21875	-5.42114	0.140607	20	244.9699	4.62	-0.3131
43	5.46	-0.48756	-0.34619	0.715961	2.739452	0.2	-4.26554	-0.41474	18	364.4208	5.20	0.2614

44	4.93	-0.47628	-0.35879	0.734753	2.744759	0.21875	-5.42114	-0.54154	20	391.6472	5.35	-0.4220
45	6.00	-0.45021	-0.3566	0.742185	2.92537	0.121212	-5.54456	-0.63642	21	390.8438	5.77	0.2321
46	5.92	-0.47322	-0.34009	0.724696	2.925081	0.121212	-5.54456	-0.33508	21	390.7534	5.72	0.1971
47	5.88	-0.50543	-0.33309	0.725162	2.925036	0.121212	-5.54456	-0.50312	21	395.551	5.64	0.2367
48	5.13	-0.43985	-0.34697	0.726749	2.924191	0.096774	-4.38896	-0.57797	19	354.7831	5.55	-0.4168
51	4.55	-0.50608	-0.40037	0.747983	2.792774	0.225806	-5.57253	-0.28617	20	389.7123	4.93	-0.3806
52	5.33	-0.5166	-0.38144	0.737511	2.7923	0.225806	-5.57253	-0.04607	20	389.6762	5.41	-0.0813
53	5.30	-0.51268	-0.37444	0.730729	2.792214	0.225806	-5.57253	-0.13285	20	391.6064	5.33	-0.0334
54	5.21	-0.47884	-0.40832	0.735546	2.790994	0.206897	-4.41693	-0.20078	18	350.9011	5.04	0.1700
56	4.87	-0.53307	-0.42304	0.765963	2.791864	0.206897	-4.26401	0.021417	18	340.02	5.01	-0.1352
58	5.69	-0.50701	-0.412	0.750792	3.034299	0.090909	-4.61058	-0.22471	25	398.6733	5.47	0.2185
60	5.29	-0.39696	-0.27355	0.776773	3.034615	0.096774	-3.35656	-0.37939	22	429.9749	5.23	0.0564
61	4.79	-0.50193	-0.43781	0.787634	3.034265	0.068966	-3.97024	-0.10717	22	402.551	4.76	0.0311
62	4.88	-0.48485	-0.41943	0.745826	3.034298	0.096774	-4.02062	-0.1516	23	428.7566	4.77	0.1099
63	4.52	-0.44583	-0.36277	0.718034	3.047983	0.09375	-4.15157	-0.22446	24	429.1572	4.57	-0.0495
64	4.52	-0.49038	-0.37638	0.700285	3.061642	0.096774	-4.42709	-0.11681	23	488.7885	4.94	-0.4189
65	4.52	-0.53808	-0.4561	0.823608	3.028354	0.066667	-4.13893	-0.51908	21	367.1241	4.92	-0.4048
67	4.52	-0.52735	-0.43351	0.783545	3.03069	0.121212	-4.25078	-0.57581	23	414.729	4.48	0.0375
68	4.52	-0.44858	-0.27355	0.67972	3.058267	0.074074	-2.23887	0.122182	17	351.7489	4.75	-0.2291
69	4.52	-0.3969	-0.27356	0.67976	3.030895	0.041667	-2.25272	-0.17549	17	362.3517	4.19	0.3275
												0.2087

71	4.52	-0.53808	-0.49986	0.854311	2.582083	0.111111	-4.3668	-0.30719	14	300.6806	4.31	
73	4.52	-0.54843	-0.34375	0.705257	2.61022	0.181818	-5.77608	-0.46157	18	380.1791	4.79	-0.2698
74	5.61	-0.49763	-0.41475	0.867923	2.587962	0.103448	-6.65421	-0.27854	17	335.5798	5.51	0.0977
75	4.52	-0.5085	-0.3597	0.719454	2.606652	0.129032	-6.57564	-1.07103	17	298.6164	4.82	-0.3039
76	4.52	-0.53808	-0.45456	0.854311	2.643398	0.16129	-6.47664	-1.6727	17	322.3822	4.63	-0.1123
78	5.76	-0.5087	-0.40627	0.92341	2.591069	0.129032	-7.14946	-1.06612	17	314.7956	5.08	0.6800
79	4.52	-0.5071	-0.34196	0.717573	2.653562	0.15625	-6.1306	-0.849	15	341.0613	4.42	0.1031
80	6.52	-0.50761	-0.43667	0.885183	2.606634	0.105263	-8.23121	-0.67945	23	378.4928	6.34	0.1828
81	4.46	-0.52308	-0.46709	0.905181	2.609082	0.166667	-6.24408	-1.06445	17	304.207	4.86	-0.3981
82	4.56	-0.49315	-0.45805	0.909364	2.608691	0.173913	-6.18813	-0.7946	18	321.3681	4.13	0.4298
83	4.27	-0.49295	-0.45743	0.936491	2.609314	0.173913	-6.62744	-0.54232	18	305.2247	4.84	-0.5710

85	4.14	-0.49312	-0.45774	0.909421	2.633948	0.153846	-5.84825	-0.54119	17	371.2936	4.32	-0.1769
86	5.00	-0.47654	-0.40829	0.92898	2.606236	0.190476	-5.02206	-0.49993	15	329.1525	4.29	0.7073
87	4.23	-0.34205	-0.28855	0.920589	2.609608	0.230769	-5.37016	-0.6221	15	400.5386	4.59	-0.3630
89	5.71	-0.51372	-0.37607	0.913362	2.750752	0.148148	-6.27911	-0.7058	18	377.1368	377.1368	0.3582
90	5.20	-0.4931	-0.45771	0.93233	2.697315	0.148148	-6.72573	-0.83967	18	382.8594	382.8594	-0.3414

S27. Experimental (Exp.pEC$_{50}$) and predicted (Pred.pEC$_{50}$) values of the training set compounds according to the developed QSAR model. The selected 2D Subdivided Surface Area, Adjacency and Partial Charge descriptors and the 3D Surface Area, Volume and Shape Descriptor values have been reported.

Cp.	Exp. pEC$_{50}$	PEOE _VSA+5	PEOE_ VSA-6	SlogP _VSA4	SlogP _VSA5	SlogP _VSA9	SMR _VSA2	SMR _VSA4	vsurf_ ID1	Vsurf _ID7	vsurf_Wp2	vsurf_Wp3	Pred. pEC$_{50}$	Residual
1	6.18	12.94953	6.788011	58.17079	37.73681	96.81097	0	51.83751	0.800828	0.493301	469.375	148.875	6.12	0.0584
4	7.88	12.94953	9.291766	58.17079	18.86841	184.3893	0	51.83751	1.128163	1.685388	472.75	159.25	7.32	0.5626
7	6.72	25.89906	17.05931	58.63956	18.86841	170.3259	0	51.83751	0.600447	1.687995	513.75	173.375	6.94	-0.2237
8	6.83	25.89906	14.97434	58.63956	50.55958	167.8393	0	70.57043	0.27258	0.752095	542.375	181.5	6.59	0.2433
9	6.33	25.89906	9.428658	57.7819	18.86841	165.5113	16.78553	51.83751	0.430511	1.366267	529.875	206.125	6.95	-0.6186
10	6.90	25.89906	9.291766	58.63956	18.86841	165.5113	16.66301	51.83751	0.565331	1.356548	523.75	197.875	7.36	-0.4613
12	6.86	12.94953	9.291766	34.34852	37.73681	165.5113	16.66301	51.83751	0.817541	1.646662	503.125	184.875	7.08	-0.2195
22	8.69	25.89906	9.291766	58.21073	18.86841	204.66	16.66301	51.83751	1.014075	1.970239	514.375	191.5	8.07	0.6208
23	8.69	25.89906	9.291766	61.39631	18.86841	198.8373	16.66301	51.83751	0.951192	1.522542	509.75	188.625	8.03	0.6621
25	7.88	25.89906	9.291766	60.96748	18.86841	198.8373	16.66301	51.83751	0.888762	1.297468	516.125	204.875	7.90	-0.0228
26	7.95	25.89906	9.291766	60.96748	18.86841	237.986	16.66301	51.83751	1.027718	1.585446	515.75	195.5	8.50	-0.5481

27	4.82	12.94953	5.144404	33.41894	70.76774	46.14079	18.01075	25.05577	0.653004	1.248182	516	123.125	4.31	0.5125
28	4.82	12.94953	5.144404	33.41894	70.76774	46.14079	18.01075	25.05577	0.731779	1.509997	521.875	128.875	4.60	0.2203
29	4.85	0	0.136891	34.77734	0	100.2576	18.01075	25.05577	0.610643	0.692451	504.125	136.875	5.18	-0.3335
33	5.22	12.94953	2.640647	36.60452	35.38387	74.22338	18.01075	25.05577	0.947415	1.384679	512.875	136.375	5.48	-0.2638
30	4.95	12.94953	2.503756	30.23337	35.38387	22.53146	12.24533	7.045022	1.173449	1.768574	473.5	80.375	5.12	-0.1726
31	5.53	12.94953	2.503756	30.23337	35.38387	46.71999	3.124314	7.045022	0.719132	1.033341	493.5	84.25	5.37	0.1581
34	5.63	12.94953	2.640647	36.60452	35.38387	74.22338	18.01075	25.05577	1.163676	1.649628	508.125	132.75	5.51	0.1183
35	5.38	12.94953	2.640647	36.60452	35.38387	74.22338	18.01075	25.05577	0.967555	0.913348	509.375	131.25	5.22	0.1587

36	5.92	12.94953	0.136891	36.17569	0	68.97995	18.01075	25.05577	0.899112	1.16417	507.5	132.75	5.14	0.7827
37	4.87	12.94953	0.136891	36.60452	0	68.97995	18.01075	25.05577	1.274256	1.278531	498.5	132.125	5.14	-0.2747
39	5.00	12.94953	0.136891	36.60452	0	68.97995	18.01075	25.05577	0.966741	0.86576	489.125	128.25	5.18	-0.1837
41	4.31	12.94953	5.144404	36.60452	70.76774	79.46681	18.01075	25.05577	1.189321	1.069763	440.75	118.125	4.62	-0.3131
43	5.46	12.94953	2.640647	36.17569	35.38387	74.22338	18.01075	25.05577	1.041974	1.364302	526.125	138.25	5.20	0.2614
44	4.93	12.94953	5.144404	36.60452	70.76774	79.46681	18.01075	25.05577	1.193353	1.539765	516.75	135.875	5.35	-0.4220
45	6.00	12.94953	2.503756	36.60452	35.38387	74.22338	3.124314	7.045022	0.906389	1.459584	485.25	93	5.77	0.2321
46	5.92	12.94953	2.503756	36.60452	35.38387	74.22338	3.124314	7.045022	0.900818	1.2158	486.375	92.625	5.72	0.1971
47	5.88	12.94953	2.503756	36.60452	35.38387	74.22338	3.124314	7.045022	0.933468	1.22687	495	89.875	5.64	0.2367
48	5.13	12.94953	0	36.17569	0	68.97995	3.124314	7.045022	0.752685	1.216956	484.75	92.375	5.55	-0.4168
51	4.55	12.94953	2.640647	36.60452	35.38387	74.22338	18.01075	25.05577	0.160016	0.717382	512.625	110.875	4.93	-0.3806
52	5.33	12.94953	2.640647	36.60452	35.38387	74.22338	18.01075	25.05577	0.558261	1.108011	522.75	128.75	5.41	-0.0813
53	5.30	12.94953	2.640647	36.60452	35.38387	74.22338	18.01075	25.05577	0.470551	0.787824	540.625	131.875	5.33	-0.0334
54	5.21	12.94953	0.136891	36.17569	0	68.97995	18.01075	25.05577	0.326577	0.776319	522.375	125.25	5.04	0.1700
56	4.87	12.94953	0.136891	36.60452	0	68.97995	18.01075	25.05577	0.701703	0.832017	529.125	126	5.01	-0.1352
58	5.69	0	2.777538	9.127897	54.25227	53.60323	53.03832	4.717102	1.188067	2.009089	510	122.5	5.47	0.2185
60	5.29	0	2.777538	10.05747	54.25227	88.28671	34.79628	4.717102	0.357714	0.54331	526	130	5.23	0.0564
61	4.79	0	0.273782	9.127897	18.86841	18.43958	34.79628	4.717102	0.498902	0.477126	490.375	113.875	4.76	0.0311
62	4.88	0	2.777538	9.127897	54.25227	23.68301	34.79628	4.717102	0.439908	0.629279	516.125	121.125	4.77	0.1099
63	4.52	0	2.640647	9.127897	87.14946	23.68301	16.78553	4.717102	0.393936	0.685366	484.125	86.75	4.57	-0.0495
														-0.4189

64	4.52	0	2.777538	10.35312	54.25227	5.243428	39.20708	4.717102	0.212023	0.722736	482.75	118	4.94	
65	4.52	12.94953	0.273782	32.99011	18.86841	0	34.79628	4.717102	0.848914	1.119773	480.375	119.375	4.92	-0.4048
67	4.52	0	2.777538	9.127897	73.12068	5.243428	34.79628	4.717102	0.449963	0.695605	527.5	128.375	4.48	0.0375
68	4.52	0	2.777538	5.942323	85.94345	5.243428	34.79628	4.717102	0.794642	2.366449	434.75	121	4.75	-0.2291
69	4.52	0	2.777538	5.942323	87.14946	5.243428	34.79628	4.717102	0.537017	1.531974	395.375	106.625	4.19	0.3275
71	4.52	12.94953	2.503756	27.04779	35.38387	7.571348	0	11.3333	0.701	0.923499	495.125	146.5	4.31	0.2087
73	4.52	12.94953	10.01502	27.04779	141.5355	23.30163	0	11.3333	0.73529	1.624358	534.25	161.25	4.79	-0.2698
74	5.61	12.94953	2.503756	27.04779	35.38387	61.68011	9.121018	11.3333	0.84081	1.107921	491.5	144.75	5.51	0.0977
75	4.52	19.64908	2.503756	30.23337	35.38387	43.65411	50.93501	14.09004	0.715313	0.807208	532.25	153.25	4.82	-0.3039
76	4.52	19.64908	2.503756	27.04779	54.25227	10.3281	50.93501	14.09004	0.61446	1.191052	581.875	166.875	4.63	-0.1123
78	5.76	19.64908	2.503756	27.04779	35.38387	49.47674	50.93501	14.09004	0.640504	0.81883	540.875	165.125	5.08	0.6800

79	4.52	12.94953	36.4348	26.61896	35.38387	100.8135	50.93501	13.66122	0.505315	0.708749	4.42	0.1031	4.42	0.1031
80	6.52	12.94953	2.503756	27.04779	35.38387	38.84904	0	20.16555	0.511739	0.588034	6.34	0.1828	6.34	0.1828
81	4.46	0	0	3.185575	33.24191	66.75472	1.550734	27.21057	0.739348	2.128536	4.86	-0.3981	4.86	-0.3981
82	4.56	0	0	0	33.24191	81.71484	10.67175	27.21057	0.286104	0.822712	4.13	0.4298	4.13	0.4298
83	4.27	0	0	0	33.24191	105.9034	1.550734	27.21057	0.587894	1.361566	4.84	-0.5710	4.84	-0.5710
85	4.14	0	5.007512	0	33.24191	77.24158	1.550734	27.21057	0.294075	0.617597	4.32	-0.1769	4.32	-0.1769
86	5.00	0	0	0	33.24191	98.03241	1.550734	24.95457	0.525247	1.002255	4.29	0.7073	4.29	0.7073
87	4.23	0	8.406116	26.61896	42.97603	100.0807	1.550734	29.47381	0.452959	0.437706	4.59	-0.3630	4.59	-0.3630
89	5.71	0	0.136891	3.185575	52.11031	69.51147	1.550734	47.97807	0.436705	0.886085	377.1368	0.3582	377.1368	0.3582
90	5.20	14.92559	0.136891	0	34.79264	125.5932	3.101468	47.97807	0.730122	0.597511	382.8594	-0.3414	382.8594	-0.3414

S28. Experimental (Exp.pEC_{50}) and predicted (Pred.pEC_{50}) values of the test set compounds according to the developed QSAR model. The selected 2D Adjacency and Distance Matrix Descriptors, Pharmacophore Feature Descriptors, Physical Properties, Atom Counts and Bond Counts descriptors and the 3D Conformation Dependent Charge Descriptors values have been reported.

Cp.	**Exp. pEC_{50}**	**BCUT_SLOGP_1**	**BCUT_SMR_1**	**BCUT_SMR_2**	**BCUT_SMR_3**	**b_1rotR**	**logS**	**dipoleY**	**a_hyd**	**ASA+**	**Pred. pEC_{50}**	**Residual**
3	6.10	-0.33047944	-0.26404753	0.73366147	2.8013721	0.13043478	-4.14505	1.025835	14	349.56198	6.47	-0.3730
6	8.39	-0.17167728	-0.11908972	0.59196395	2.9551604	0.11111111	-5.4538898	1.0793978	18	416.81415	8.50	-0.1134
11	8.52	-0.2496783	-0.14757159	0.60403872	2.9551349	0.11538462	-3.9227901	1.0493044	15	352.38104	7.60	0.9194
24	8.52	-0.21303622	-0.1171928	0.5663017	2.9551418	0.1	-5.1322598	0.47866929	19	354.41968	7.96	0.5565

32	5.30	-0.47616071	-0.36629966	0.80957109	2.9251747	0.125	-5.6871099	0.31962168	20	390.99222	5.67	-0.3738
38	5.00	-0.53411287	-0.42294818	0.76985401	2.7408793	0.17857143	-4.0622401	0.090998821	17	314.42032	4.92	0.0811
40	4.25	-0.50695312	-0.33814892	0.72322482	2.7434282	0.21875	-5.4211402	-0.35460791	20	369.87402	5.03	-0.7757
55	4.79	-0.5048244	-0.41092402	0.74816161	2.7917297	0.20689656	-4.26401	0.043317597	18	341.32532	5.08	-0.2927
57	5.00	-0.50591195	-0.34110171	0.69058079	3.0343418	0.12121212	-4.0710001	-0.099414699	24	451.85364	4.62	0.3786
59	5.58	-0.50857282	-0.41164595	0.75098193	3.034306	0.090909094	-4.61058	-0.23075099	25	399.97519	5.23	0.3450
66	4.52	-0.50590354	-0.33911341	0.68981081	3.0312951	0.11111111	-2.6305399	-0.617037	18	383.77551	4.33	0.1878

72	5.44	-0.52836478	-0.46312457	0.81207639	2.5848756	0.10714286	-5.91992	-0.3858822	16	307.17242	4.96	0.4835
77	4.52	-0.50872862	-0.36945948	0.8581714	2.5899618	0.12903225	-7.1494598	-0.35955641	17	324.83478	5.28	-0.7613
84	5.19	-0.49309871	-0.45771432	0.93088794	2.6487799	0.14814815	-6.67063	-0.80477411	17	343.14407	5.12	0.0659
88	4.49	-0.34952211	-0.29147619	0.93386561	2.6100163	0.18181819	-6.24999	-0.531663	17	384.87665	5.60	-1.1057

S29. Experimental (Exp.pEC_{50}) and predicted (Pred.pEC_{50}) values of the test set compounds according to the developed QSAR model. The selected 2D Subdivided Surface Area, Adjacency and Partial Charge descriptors and the 3D Surface Area, Volume and Shape Descriptor values have been reported.

Cp.	**Exp. pEC_{50}**	**PEOE _VSA+5**	**PEOE_ VSA-6**	**SlogP _VSA4**	**SlogP _VSA5**	**SlogP _VSA9**	**SMR _VSA2**	**SMR _VSA4**	**vsurf_ ID1**	**Vsurf _ID7**	**vsurf_Wp2**	**vsurf_Wp3**	**Pred. pEC_{50}**	**Residual**
3	6.10	12.949531	9.2917662	58.170788	18.868406	117.73722	0	51.837513	1.4823005	1.6377909	459.875	149.625	6.47	-0.3730
6	8.39	12.949531	9.2917662	58.170788	18.868406	230.11502	0	51.837513	1.0830811	1.896114	480.875	162.625	8.50	-0.1134
11	8.52	25.899061	9.2917662	58.210732	18.868406	165.51132	16.663008	51.837513	0.84125829	1.6844577	517.75	199.375	7.60	0.9194
24	8.52	25.899061	9.2917662	60.96748	18.868406	210.39166	24.422523	51.837513	1.641968	0.92884934	507.25	209	7.96	0.5565
32	5.30	12.949531	2.503756	30.233366	38.438972	53.52544	6.1794186	7.0450215	0.92542022	1.2124147	506.125	83.875	5.67	-0.3738
38	5.00	12.949531	0.13689101	36.604515	0	68.97995	18.01075	25.055773	1.0961233	0.84826136	502.25	132.5	4.92	0.0811
40	4.25	12.949531	5.1444035	36.604515	70.767738	79.466805	18.01075	25.055773	1.2389504	1.0051649	500.375	131.625	5.03	-0.7757
55	4.79	12.949531	0.13689101	36.604515	0	68.97995	18.01075	25.055773	0.69999182	0.85419071	525.75	125.625	5.08	-0.2927
57	5.00	0	5.2812943	9.1278973	89.636139	28.926434	34.79628	4.7171016	0.26172695	0.41990376	527.75	127.625	4.62	0.3786
		0	2.7775381	9.1278973	54.252274	53.603233	53.038315	4.7171016	0.90120083	1.5566729	508.625	122	5.23	0.3450

59	5.58													
66	4.52	0	2.7775381	5.9423227	54.252274	38.569443	34.79628	4.7171016	0.70693582	1.4608345	430	115.125	4.33	0.1878
72	5.44	12.949531	2.503756	27.047791	35.383869	22.531462	9.1210184	11.333296	0.81351507	1.249822	484	147.25	4.96	0.4835
77	4.52	19.649082	2.503756	27.047791	35.383869	49.476738	50.935009	14.090043	0.6767658	0.71812558	540.875	163	5.28	-0.7613
84	5.19	0	0	0	33.241909	98.617111	1.5507339	47.978065	0.68520218	0.61810213	524.25	138.625	5.12	0.0659
88	4.49	0	0	0	33.241909	137.18106	1.5507339	25.383394	0.48546532	1.3971066	448.5	96.375	5.60	-1.1057

S30. Distribution of the b_1RotR (*up*) and a_hyd (*down*) descriptor values with respect to the experimental (Exp.pEC$_{50}$) potency data of the dataset compounds (shown as white dots).

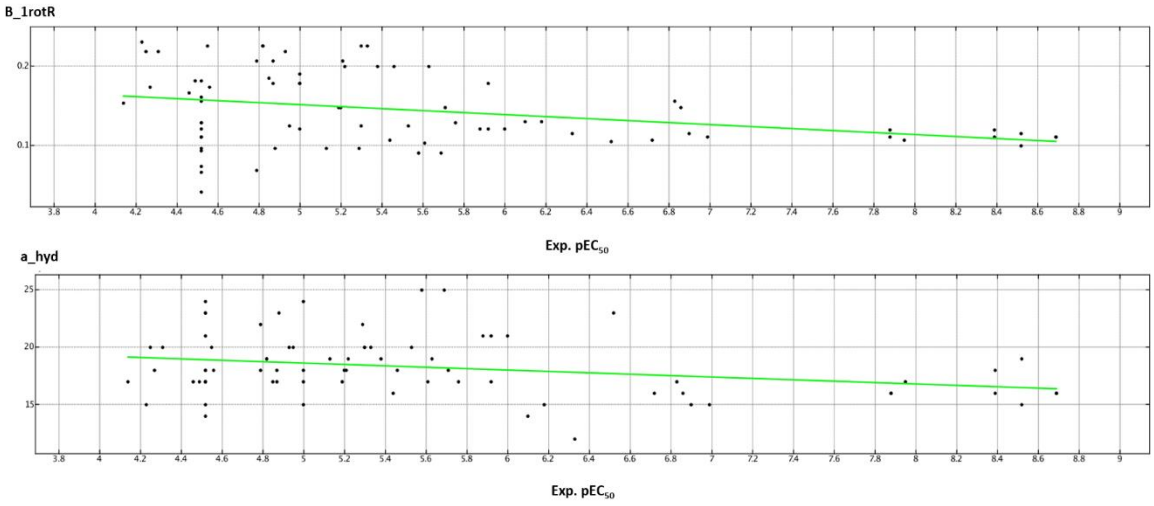

S31. Distribution of the ASA$^+$ (*up*), LogS and BCUT_SMR3 (*down*) descriptor values with respect to the experimental (Exp.pEC$_{50}$) potency data of the dataset compounds (shown as white dots).

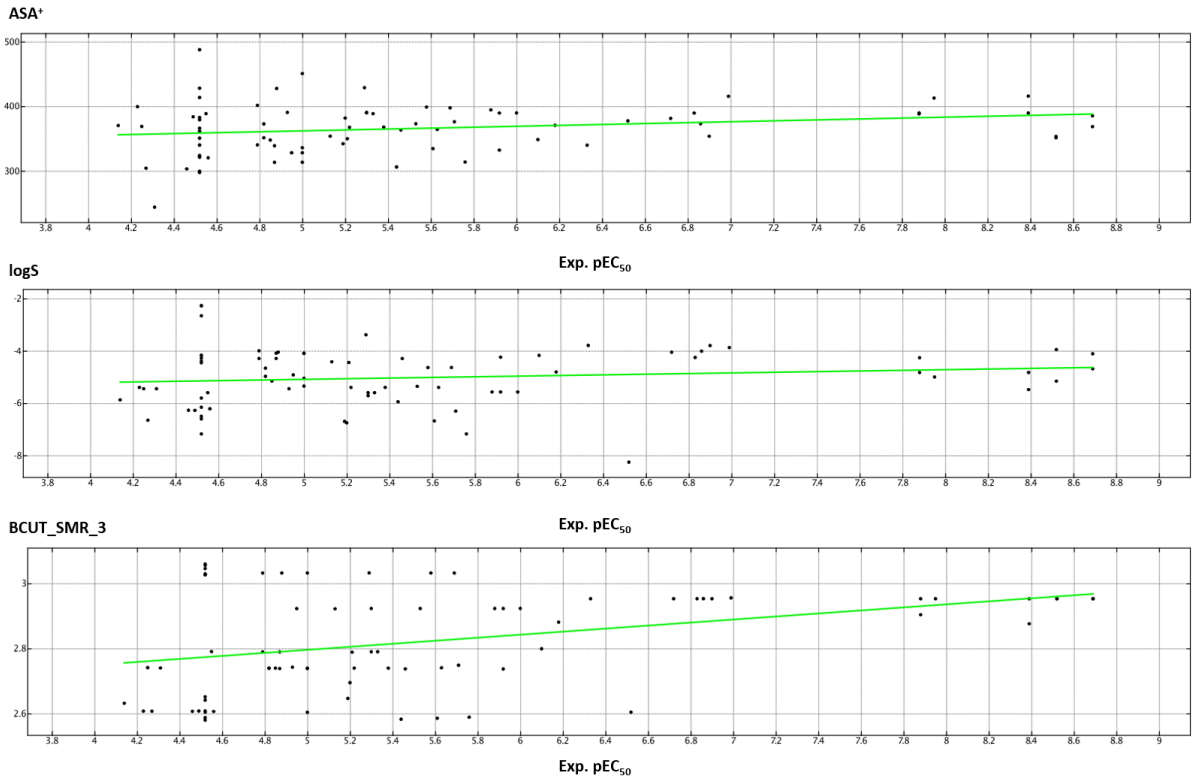

S32. Pattern of the most important interactions within the CFTR protein observed for the most promising GLPG1837 analogues (pEC_{50} = 7.88-9.26).

Potentiator	H-bonds		π-π stacking		Cation - π		Van der Waals	
	Amino acid residues	Ligand portion	Amino acid residues	Ligand portion	Amino acid residues	Ligand portion	Amino acid residues	Ligand portion
4	F931	oxygen atom of carbonyl moiety	F312	Thienopyran -based core	R933	Thienopyran -based core	A309	Thienopyran -based core
	Y304	Primary amide group						
	F932	Hydroxy l group of phenol ring						
5	F931	Two oxygen atoms of carbonyl moieties	F305 F312	Thienopyran -based core	R933	Thienopyran -based core	A309	Thienopyran -based core
	Y304	Primary amide group						
	F932	Hydroxy l group of phenol ring						
6	F931	Two oxygen atoms of carbonyl moieties	F305 F312	Thienopyran -based core	R933	Thienopyran -based core	A309	Thienopyran -based core
	Y304	Primary amide group						
	F932	Oxygen atom of amide group						
11	F931	Two oxygen atoms of carbonyl moieties	F931 F932	Pyrazole ring			F236 F305 F312	Thienopyran -based core
	Y304	Primary amide group	F236 F305 F312	Thienopyran -based core				
	R933	Pyrazole ring						
20	F931	Two oxygen atoms of carbonyl moieties	F931 F932	Pyrazole ring			F236 F305 F312	Thienopyran -based core

	Y304	Primary amide group	F236 F305 F312	Thienopyran -based core				
	R933	Hydroxy l group						
21 (*S enantiomer)*	F932 Y304 S308	Two oxygen atoms of carbonyl moieties	F236 F305 F312	Thienopyran -based core			F236 F305 F312	Thienopyran -based core
	R933	Alkoxy group						
22	F931	Two oxygen atoms of carbonyl moieties	F932 F931	4-Cl-1H-pyrazole				
	Y304	Primary amide group	F236 F305 F312	Thienopyran -based core				
	R933	Alkoxy group						
23	F931	Two oxygen atoms of carbonyl moieties	F932 F931	3-methyl-1H-Pyrazole			F236 F305 F312	Thienopyran -based core
	Y304	Primary amide group	F236 F305	Thienopyran -based core				
	R933	Alkoxy group						

S33. Pattern of the most important interactions within the CFTR protein observed for the most promising CQs (pEC_{50} = 4.55-5.92).

Potentiator	**H-bonds**		**π-π stacking**		**Cation - π**		**Van der Waals**	
	Amino acid residues	Ligand portion	Amino acid residues	Ligand portion	Amino acid residues	Ligand portion	Amino acid residues	Ligand portion
30	F931	Methoxy group	F236	2-F-phenyl ring			F236 L233	Piperazine ring
	R933	Benzoyl moiety	F305 F312 Y304	Cyanoquinoline core				
31	F931	Methoxy group	F236	2-Cl-phenyl ring			F236 L233	Piperazine ring
	R933	Benzoyl moiety	F305 F312 Y404	Cyanoquinoline core				
32	F931	Methoxy group	F236	2-Br-phenyl ring			F236 L233	Piperazine ring
	R933	Benzoyl moiety	F305 F312 Y304	Cyanoquinoline core				

34	F931	Nitrogen atom of quinoline core	F236	o-Methoxy-benzoyl moiety				
	R933	Benzoyl moiety	F312 F931	Cyanoquinoline core				
35	F931	Nitrogen atom of quinoline core	F236	p-Methoxy-benzoyl moiety				
	R933	Benzoyl moiety	F312 F931	Cyanoquinoline core				
45	F931	Nitrogen atom of quinoline core	F931 F312	Cyanoquinoline core	R933	Methoxy-benzoyl moiety	F236 L233	Piperazine ring
	R933	Benzoyl group	F236	o-Methoxy-Benzoyl moiety				
46	F931	Nitrogen atom of quinoline core	F236	m-Methoxy-Benzoyl moiety	R933	Methoxy-benzoyl moiety	F236 L233	Piperazine ring
	R933	Benzoyl group	F312 F931	Cyanoquinoline core				
47	F931	Nitrogen atom of quinoline core	F236	p-Methoxy-Benzoyl ring	R933	Methoxy-benzoyl moiety	F236 L233	Piperazine ring
	R933	Benzoyl group	F312 F931	Cyanoquinoline core				
53	F931	Nitrogen atom of quinoline core	Y304 F236 F305	Cyanoquinoline core				
	R933	Benzoyl group						

S34. Pattern of the most important interactions within the CFTR protein observed for the most promising tetrahydropyridoindole derivatives (pEC_{50} = 5.00-5.58).

Potentiator	**H-bonds**		**π-π stacking**		**Cation - π**		**Van der Waals**	
	Amino acid residues	Ligand portion	Amino acid residues	Ligand portion	Amino acid residues	Ligand portion	Amino acid residues	Ligand portion
57	R933	Methoxy group	F236 Y304 F305	m-methoxy benzyl moiety	F931	Protonated nitrogen atom of tricyclic system	A309	m-methoxy benzyl moiety
58	R933	Methoxy group	F236 F305 Y304	2,4-di-F benzyl moiety	F931	Protonated nitrogen atoms of tricyclic system	A309	2,4-di-F benzyl moiety
59	R933	Methoxy group	F236 F305 Y304	3,4-di-F benzyl moiety	F931	Protonated nitrogen atoms of tricyclic system	A309	3,4-di-F benzyl moiety
64	R933	Methoxy group	F932 F305	Tricyclic system				

S35. Pattern of the most important interactions within the CFTR protein observed for the most promising pyrazoloquinolines analogues (pEC_{50} = 5.44-6.52).

Potentiator	H-bonds		π-π stacking		Cation - π		Van der Waals	
	Amino acid residues	Ligand portion	Amino acid residues	Ligand portion	Amino acid residues	Ligand portion	Amino acid residues	Ligand portion
74	F931	Pyrazole ring	F236	2-Cl-4-F-			F312	2-Cl-4-F-
	M929 S308	Primary amine group	Y304 F305	benzoyl moiety			F932	benzyl moiety
	R933	Methoxy group						
78	F931	Nitrogen of tricyclic core	F236 Y304 F305	2-Cl-4-nitro-phenyl group				
	M929 S308	Primary amine group						
	R933	Nitro-group						
80	R933	Aromatic quinoline substituent	Y304 F305 F312 F316	Aromatic quinoline substituent	R933	Methoxy -group		

S36. Pattern of the most important interactions within the CFTR protein observed for the most promising AATs (pEC_{50} = 4.56-5.71).

Potentiator	H-bonds		π-π stacking		Cation - π		Van der Waals	
	Amino acid residues	Ligand portion	Amino acid residues	Ligand portion	Amino acid residues	Ligand portion	Amino acid residues	Ligand portion
82	F931	Thiazole nitrogen atom	F932	4-F-phenyl group			F305 F312	Aminoaryl-moiety
	Y304	Amine group	F312 F305	Aminoaryl-moiety				
84	R933	Carbamate moiety	F305	Benzoxalone ring				
	F931	Thiazole nitrogen atom	F312	Thiazole ring				
86	F931	Thiazole nitrogen atom	F932	Thiazole ring				
	Y304	Amine group						

S37. Comparison of the CQ **45** (*left*; *C* atom in green) and **50** (*right*; *C* atom in yellow) docking positioning with the pharmacophore model built onto the thienopyranes. Potentiator **11** is depicted as reference compound (*C* atom; white).

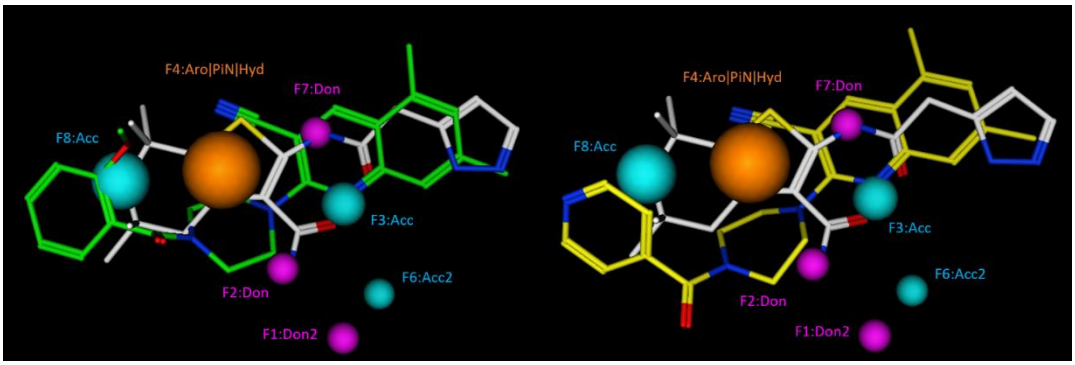

S38. Comparison of the pyrazolquinolines **80** (*left*; *C* atom in orange) and **71** (*right*; *C* atom in yellow) docking positioning with the pharmacophore model built onto the thienopyranes. Potentiator **11** is depicted as reference compound (*C* atom; white).

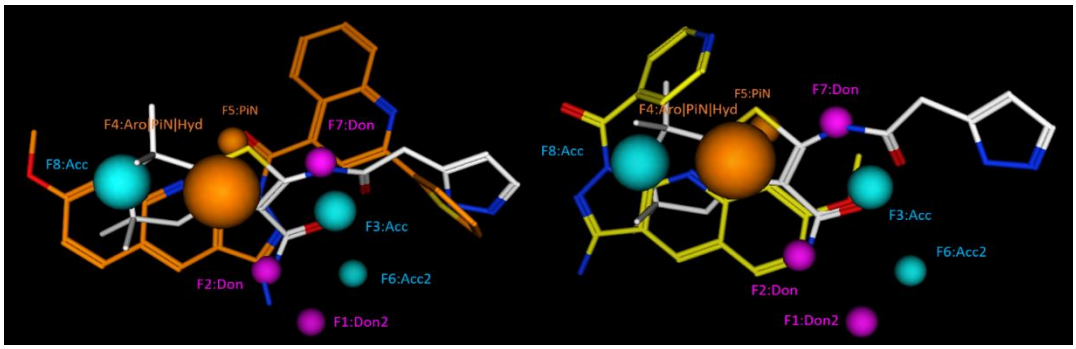

S39. Comparison of the AAT **89** (*left*; *C* atom in green) and **82** (*right*; *C* atom in green) docking positioning with the pharmacophore model built onto the thienopyranes. Potentiator **11** is depicted as reference compound (*C* atom; white).

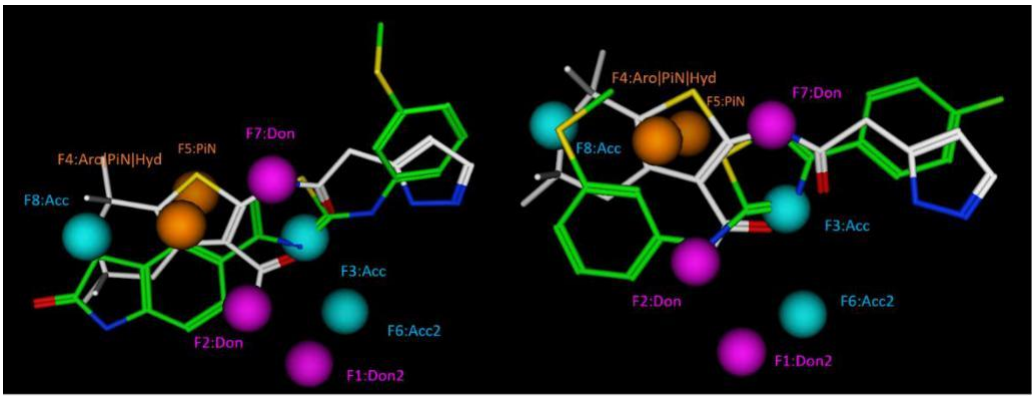

S40. Chemical structures of thiazole derivatives **91-106** as F508del-CFTR potentiators [40].

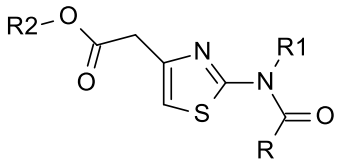

Compound	R	R_1	R_2
91	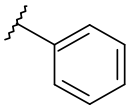	H	CH_2CH_3
92	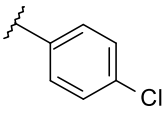	H	CH_2CH_3
93	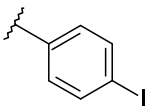	H	CH_2CH_3
94	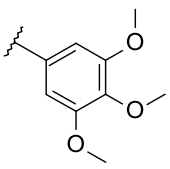	H	CH_2CH_3
95	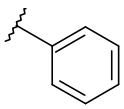	H	H
96	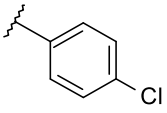	H	H
97	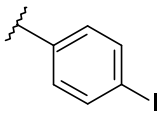	H	H

98	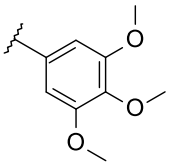	H	H
99	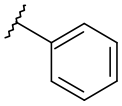	CH_2CH_3	CH_2CH_3
100	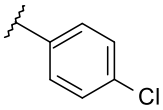	CH_2CH_3	CH_2CH_3
101	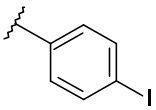	CH_2CH_3	CH_2CH_3
102	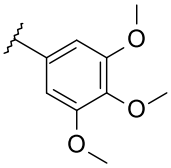	CH_2CH_3	CH_2CH_3
103	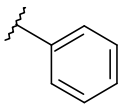	CH_2CH_3	H
104	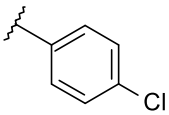	CH_2CH_3	H
105	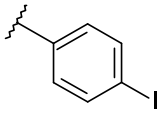	CH_2CH_3	H
106	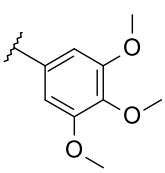	CH_2CH_3	H

S41. Chemical structures of aminoarylthiazoles **107-111** [22-23].

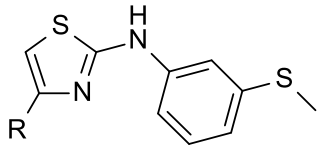

Compound	R
107	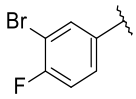
108	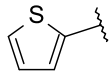
109	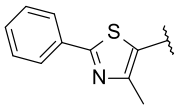
110	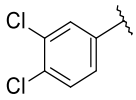
111	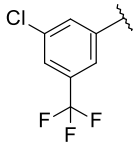

S42. Chemical structures of aminoarylthiazoles derivatives **112-139** [25].

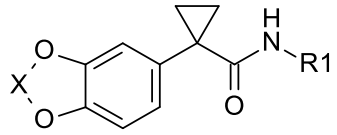

Compound	X	R_1
112	-CH_2	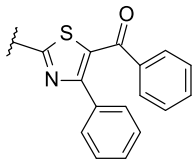
113	-CH_2	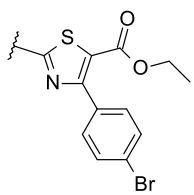

114	-CH_2	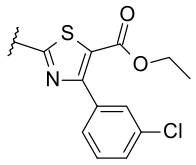
115	-CH_2	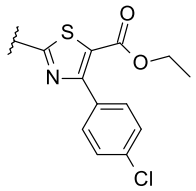
116	-CH_2	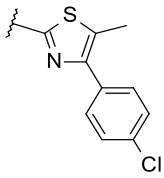
117	-CH_2	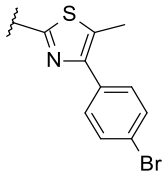
118	-CH_2	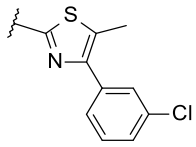
119	-CH_2	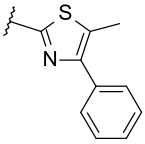
120	-CH_2	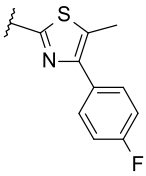
121	-CH_2	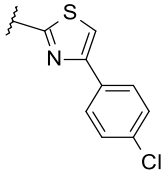
122	-CH_2	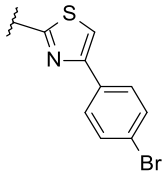
123	-CH_2	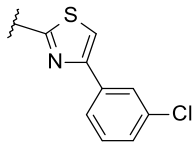

124	-CH_2	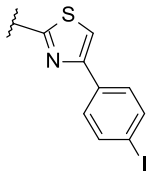
125	-CH_2	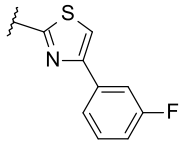
126	-CH_2	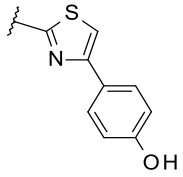
127	-CH_2	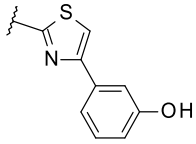
128	-CH_2	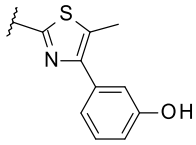
129	-CH_2	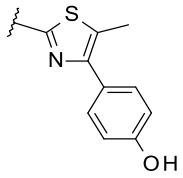
130	-CH_2	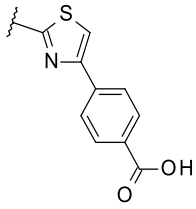
131	-CH_2	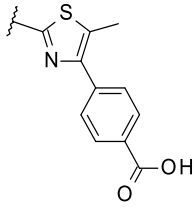
132	-CH_2	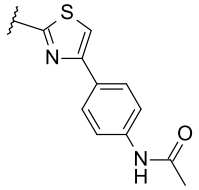

133	-CF_2	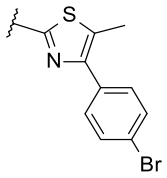
134	-CF_2	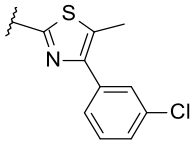
135	-CF_2	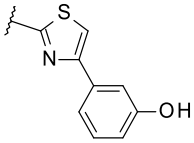
136	-CF_2	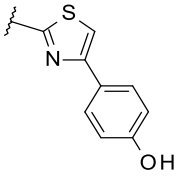
137	-CF_2	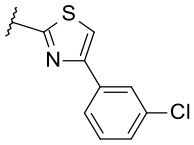
138	-CH_2	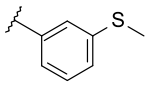
139	-CH_2	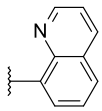

S43. Ligplot of the calculated docking mode of **100** and **101** within the CFTR cavity.

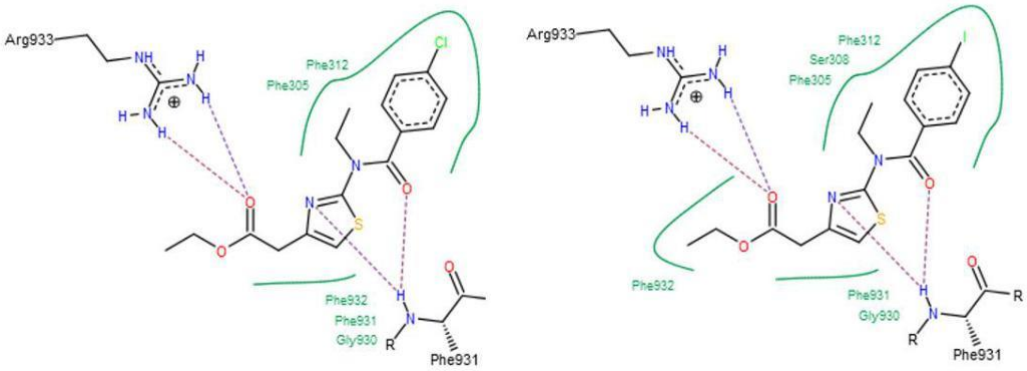

S44. Docking positioning of compound **100** (*C* atom; cyan) and **101** (*C* atom; green) at the CFTR protein in presence of VX-770 (*C* atom; magenta).

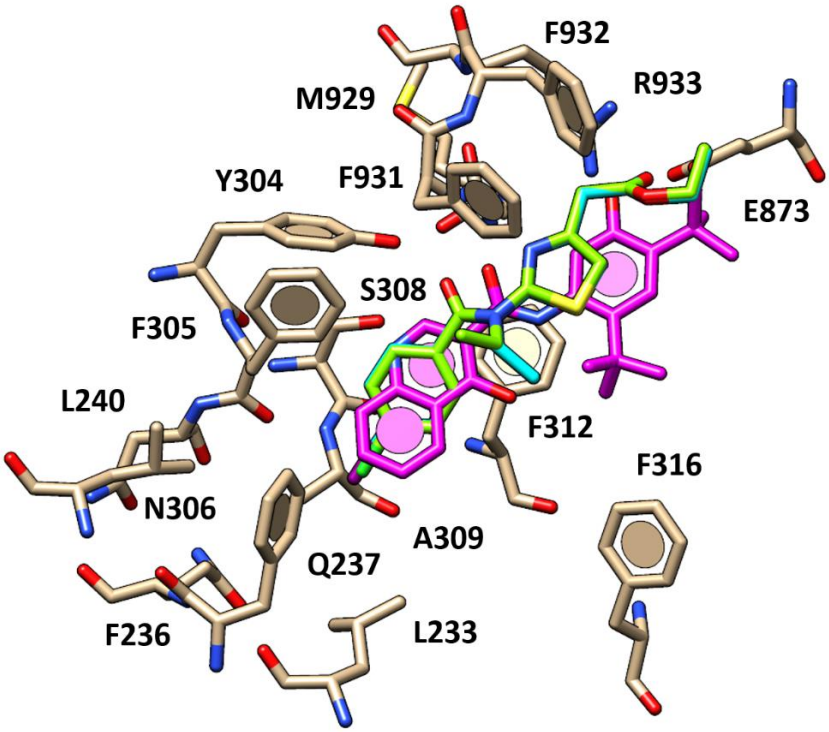

S45. Docking mode of **127** (*C* atom; green) within the CFTR cavity compared to that of VX-770 (*C* atom; magenta).

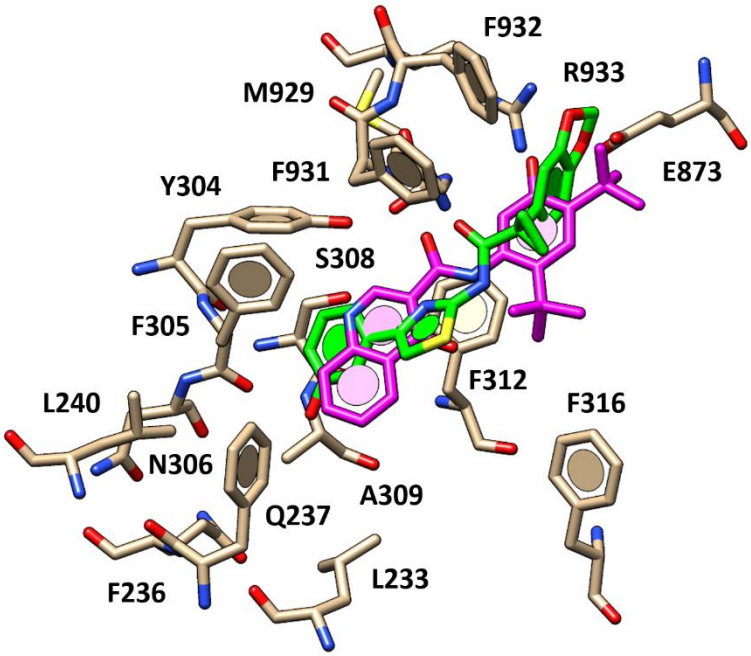

S46. Docking positioning of compound **139** (*C* atom; yellow) compared to that of VX-770 (*C* atom; magenta).

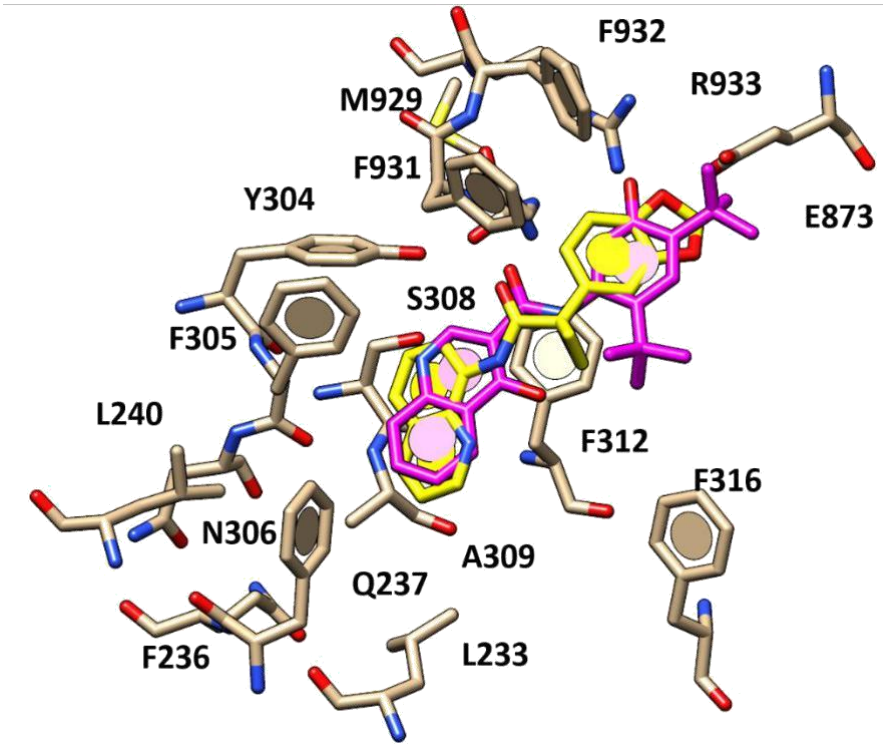

S47. Comparison of the thiazole **100** (*left*; *C* atom in coral) and **127** (*right*; *C* atom in green) with the potentiator **11** (*C* atom; white), depicted as reference compound, within the developed pharmacophore model.

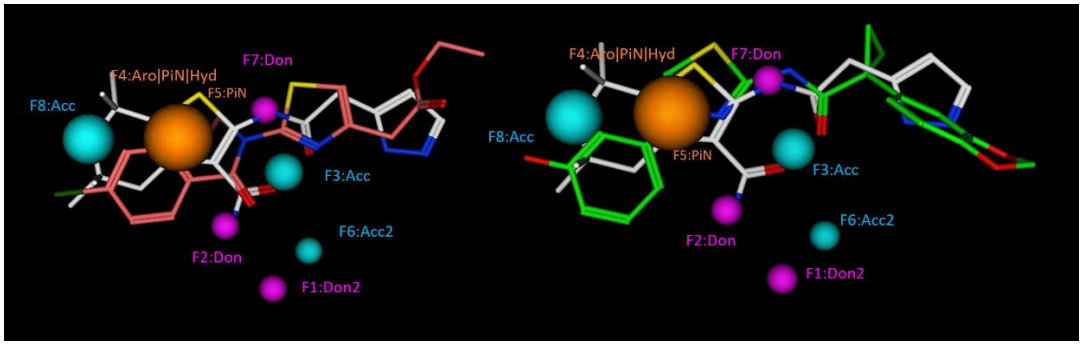

S48. Predicted pEC_{50} values of compounds **91**-**139** as putative F508del-CFTR potentiators, calculated by means of the developed QSAR model. Those compounds described in the literature as potentiators are shown in italic, blue colored. All the other compounds proved to be inactive.

Compound	Pred. pEC_{50}
91	3.76
92	4.18
93	4.35
94	3.56
95	2.82
96	3.44
97	3.47
98	2.65
99	4.04
100	5.02
101	5.21
102	4.33
103	3.11
104	3.77
105	3.74
106	2.96
107	4.06
108	4.02
109	4.04
110	4.09
111	3.96
112	4.07
113	4.09
114	4.23
115	4.24
116	3.89
117	4.16
118	3.99
119	3.48
120	3.24
121	3.49
122	3.72
123	4.58
124	3.82
125	3.97
126	4.02
127	4.87
128	5.31
129	3.27
130	3.90
131	4.23
132	3.00
133	3.00
134	3.62
136	4.02

135	4.17
136	3.66
137	4.09
138	3.57
139	4.72